https://doi.org/10.5194/egusphere-2026-2472
Preprint. Discussion started: 13 May 2026

Molecular characteristics and formation pathways of organosulfur compounds: a comparative field study across contrasting atmospheric environments

Dongmei Cai[1,2,3], Xianda Gong[1,2]*, Runqi Zhang[3], Shenyan Zhang[4], Yuhan Cheng[1,2,], Saidur Rahaman[1,2,], Yin Fang[4], Jianmin Chen[3]*

[1]*Key Laboratory of Coastal Environment and Resources of Zhejiang Province, School of Engineering, Westlake University, Hangzhou, Zhejiang 310030, China*
[2]*Research Center for Industries of the Future, Westlake University, Hangzhou, Zhejiang 310030, China*
[3] *Shanghai Key Laboratory of Atmospheric Particle Pollution and Prevention (LAP3), IRDR ICoE on Risk Interconnectivity and Governance on Weather/Climate Extremes Impact and Public Health, Department of Environmental Science and Engineering, Fudan University, Shanghai 200438, China*
[4]*State Key Laboratory of Estuarine and Coastal Research, Institute of Eco-Chongming, Blue Carbon Science and Technology Centre, East China Normal University, Shanghai, 200241, China*

Correspondence: Xianda Gong (gongxianda@westlake.edu.cn) and Jianmin Chen (jmchen@fudan.edu.cn)

*Corresponding author.

https://doi.org/10.5194/egusphere-2026-2472
Preprint. Discussion started: 13 May 2026

Abstract. Organosulfur compounds (OrgSs), especially organosulfates (OSs), are ubiquitous aerosol components. However, the spatial, seasonal, and diurnal variations of OrgS formation in polluted atmospheres remain poorly understood. Here, we monitored particulate OrgSs at an urban site and a suburban site in Shanghai and examined their molecular composition and formation pathways under contrasting atmospheric conditions. A total of 1964, 1914, and 2689 OrgS molecular formulas were detected in suburban summer, urban summer, and urban winter, respectively. More than 79% of sulfur-containing molecular formulas had $(4s + 3n)/o \leq 1$, indicating that OrgSs were dominated by OSs and nitrooxy-OSs (NOSs). Compared with summer, wintertime OrgSs exhibited lower O/C ratios but higher double-bond equivalence and aromaticity, suggesting a stronger influence of anthropogenic emissions and more unsaturated molecular structures. Although OrgSs were mostly present in aliphatic molecular structures, an increase in the number of aromatic OSs in winter revealed an enhanced contribution from anthropogenic sources. Isoprene/monoterpene-derived OSs peaked during the daytime due to photochemical oxidation in summer, whereas monoterpene-derived NOSs were markedly enhanced at night via nighttime NO_3-initiated oxidation. Non-metric multidimensional scaling analysis further revealed that OrgS composition in summer was associated with temperature and O_3 during the day but shifted toward RH-driven processing at night. In winter, inorganic nitrogen and sulfur species, aerosol liquid water content, and particle acidity became more important in shaping OrgS composition, suggesting enhanced aqueous-phase and acid-catalyzed formation. These findings provide molecular-level insights into the sources and formation of atmospheric OrgSs across contrasting environments.

https://doi.org/10.5194/egusphere-2026-2472
Preprint. Discussion started: 13 May 2026

1. Introduction

Organosulfur compounds (OrgSs) are ubiquitous in the atmosphere, spanning diverse environments from remote regions to highly polluted urban areas (Cai et al., 2020; Thomas et al., 2025; Yang et al., 2024; Zhang et al., 2025). They have been recognized as an important component in ambient $PM_{2.5}$ (up to 50%) (Lukacs et al., 2009; Surratt et al., 2008; Tolocka & Turpin, 2012), and have critical influences on aerosol physicochemical properties, such as acidity, hygroscopicity, and volatility (Fan et al., 2022b; Hansen et al., 2015). OrgSs exhibit notable chemical stability and environmental persistence, including organosulfates (OSs), sulfoxides, sulfonates, and sulfones, among which OSs have been identified as the most abundant class (Cai et al., 2020; Jiang et al., 2022; Wang et al., 2018b). Emerging evidence has underscored the hygroscopicity, light absorption, and potential toxicity of OSs (Fan et al., 2022b; Hansen et al., 2015; Jiang et al., 2025), further highlighting the critical need for in-depth investigations into the composition, sources, and formation pathways of atmospheric OrgSs.

Although OrgSs can be directly emitted from the combustion of fossil fuels and biomass, they are mainly formed through heterogeneous or multiphase reactions of sulfur dioxide (SO_2) and sulfate particles with anthropogenic and biogenic volatile organic compounds (BVOCs) (Bruggemann et al., 2020; Tang et al., 2020b). The acid-catalyzed ring-opening of epoxides in the presence of sulfuric acid seeds has been widely invoked to explain OS formation (Cai et al., 2020; Jiang et al., 2022). Additionally, OSs may be formed by sulfate radical-induced oxidation of unsaturated compounds (Noziere et al., 2010; Schindelka et al., 2013), nucleophilic substitution of tertiary organonitrates with sulfate (Darer et al., 2011), and sulfate esterification of alcohols or epoxides (Minerath et al., 2008; Minerath & Elrod, 2009). Direct formation of OSs from uptake of gaseous SO_2 by unsaturated fatty acids and organic peroxides (Shang et al., 2016; Ye et al., 2018), as well as from reactions between sulfite/sulfate ion radicals and unsaturated carbonyl compounds in the presence of Fe^{3+}, have also been reported (Huang et al., 2018). Furthermore, nighttime NO_3-initiated oxidation of BVOCs is recognized as a crucial formation pathway of nitrooxy-organosulfates (NOSs) (Hamilton et al., 2021; Surratt et al., 2008; Wang et al., 2018b). The presently proposed formation pathways presumably explain the large variety and ubiquity of OSs. However, the chemical composition of OrgSs in the actual atmosphere is highly complex, and the atmospheric relevance of these processes has yet to be fully elucidated.

The formation of OSs is strongly influenced by anthropogenic sulfate, NO_x, BVOCs, and ambient conditions, such as, relative humidity (RH) and aerosol physical

https://doi.org/10.5194/egusphere-2026-2472
Preprint. Discussion started: 13 May 2026

properties. As these factors vary across different atmospheric environments, field observations are indispensable for validating mechanistic insights from chamber experiments and uncovering previously unrecognized environmental factors. Shanghai, a coastal megacity in the Yangtze River Delta (YRD) region of China, provides a unique environment for investigating the formation and evolution of particulate OrgSs because its atmospheric environment is shaped by strong local emissions, regional transport, and pronounced seasonal meteorological contrasts. This region is characterized by high emissions of VOCs and gaseous pollutants (e.g., NO_x and SO_2), together with generally high RH and strong oxidizing capacity, which can foster complex biogenic-anthropogenic interactions (Cai et al., 2020; Han et al., 2023b; Yang et al., 2023). Furthermore, urban and suburban environments differ in emission intensity and precursor composition. These spatial and seasonal contrasts create favorable conditions for examining how anthropogenic–biogenic interactions regulate OrgS formation. Although several studies have reported the concentrations and potential formation mechanisms of biogenic VOC-derived OSs in the YRD, these OSs represented only a small fraction of total particulate OrgSs in ambient aerosols (Wang et al., 2021b; Yang et al., 2023). Therefore, a better understanding of the molecular characteristics, formation mechanisms, and key influencing factors of OrgSs in Shanghai is crucial for elucidating their role in particulate pollution and developing effective strategies to mitigate secondary organic aerosol (SOA) concentrations.

In this study, we used ultra-high performance liquid chromatography coupled with an Orbitrap mass spectrometer (UHPLC-Orbitrap MS) to characterize particulate OrgSs in Shanghai, based on field campaigns conducted at a suburban site in summer and at an urban site in both summer and winter. This strategic sampling captures the spatial, seasonal, and diurnal variability of OrgSs under contrasting atmospheric conditions. Our main objective was to unravel the spatiotemporal evolution, formation pathways, and key drivers of OrgSs at the molecular level, by comparing their compositional and structural characteristics across summer versus winter, day versus night, and low versus high sulfate and NO_x levels. This work provides molecular-level insights into organosulfur chemistry and is pivotal for assessing the role of anthropogenic pollutants in driving SOA formation in biogenically influenced urban regions.

2. Materials and methods

2.1 Aerosol sampling and site description

Ambient $PM_{2.5}$ sampling was conducted in both the urban center of Shanghai (Fudan University, Yangpu Jiangwan Campus; 31.344°N, 121.518°E) and a suburban

https://doi.org/10.5194/egusphere-2026-2472
Preprint. Discussion started: 13 May 2026

area (Qingpu Dianshan Lake; 31.136°N, 121.092°E). The urban site is representative of typical urban environments, characterized by high population density and heavy traffic emissions. The suburban site, located approximately 62 km northeast of the urban site, is influenced by a mix of regional pollutant transport and local biogenic emissions. Sampling campaigns were carried out during summer (July 22 to August 5, 2023) and winter (January 9 to 20, 2024) at the urban site, and during summer (July 22 to August 2, 2023) at the suburban site. Sampling was conducted separately during daytime (07:00−18:30) and nighttime (19:00−06:30) to capture the diurnal variations in the formation of OrgSs. All $PM_{2.5}$ samples were collected onto pre-baked quartz fiber filters (Whatman Inc.) using high-volume samplers (TH-1000C, Tianhong, China) at a flow rate of 1.05 m^3/min. Additionally, 11.5-hour field blank samples were also collected by turning off the sampling pump. A total of 60 $PM_{2.5}$ samples and 4 field blank samples were obtained from the urban site, while 30 $PM_{2.5}$ samples and 2 field blank samples were collected from the suburban site. All filter samples were stored at −20°C before analysis. The real-time monitoring of O_3、NO、NO_2, and meteorological parameters was also conducted during each sampling campaign (Table S1).

2.2 Chemical analysis and prediction of aerosol acidity and ALW

A 24 cm^2 aliquot was excised from each $PM_{2.5}$ filter sample and subjected to ultrasonic extraction three times, each with 3 mL of methanol for 30 min. The combined extracts were filtered through a 0.45 μm PTFE syringe filter to remove insoluble particles, then concentrated to near dryness under a gentle stream of nitrogen. The residue was reconstituted in 80 μL of methanol containing internal standards (IS, 200 ppb D_{17}-Octyl sulfate). The resulting solution was centrifuged at 10,000 rpm for 10 min, and the supernatant was collected for subsequent mass spectrometry analysis.

Sample extracts were analyzed using an ultra-high performance liquid chromatography system coupled with an Orbitrap Exploris 120 mass spectrometer (UHPLC-Orbitrap MS, Thermo Scientific, Germany). The electrospray ionization source was operated in negative ionization mode with the following settings: capillary temperature of 320°C, auxiliary gas flow at 10 units, sheath gas flow at 35 units, sweep gas flow at 2 units, and spray voltage at 3.0 kV. The scan range was m/z 60–900, with a resolution of 120,000 at *m/z* 200. Chromatographic separation was performed on an Acquity UPLC HSS T3 column (1.8 μm, 100 mm × 2.1 mm, Waters) with a C18 guard column (HSS T3, 1.8 μm). The flow rate was set to 0.3 mL/min, the column temperature was maintained at 40°C, and the injection volume was 5 μL. The mobile phase used a binary gradient, with solvent A as 0.1% formic acid in water and solvent B as 0.1% formic acid in acetonitrile. The gradient program was as follows: 10% B was held for

https://doi.org/10.5194/egusphere-2026-2472
Preprint. Discussion started: 13 May 2026

2 min, linearly increased to 30% B over 2−25 min, further increased to 90% B over 25−50 min, held at 90% B for 10 min (50−60 min), then decreased to 10% B over 60−61 min, followed by a 9 min column re-equilibration at 10% B prior to the next injection. External mass calibration was performed every three days using a commercial calibration solution (Ultramark 1621, Thermo Fisher, Germany) covering an m/z range of 74−1922. Due to the limited volume of the final extract (80 µL), duplicate injections were not performed. Instead, the remaining sample solution from the first injection was retained for potential targeted analyses rather than systematic re-injection. All chromatographic peaks exhibited typical Gaussian shapes, indicating satisfactory column performance and separation efficiency. Field blank samples were extracted and analyzed following the same procedure to account for potential background contamination.

Organic carbon (OC) and elemental carbon (EC) were determined using a thermal/optical carbon analyzer (DRI model 2001, Desert Research Institute, USA) with the well-established IMPROVE-A thermal/optical reflectance protocol. Organic matter (OM) was calculated by multiplying the OC by 1.6 (Liu et al., 2018; Turpin & Lim, 2001; Xing et al., 2013). Water-soluble inorganic ions (e.g., SO_4^{2-}, NO_3^-, Cl^-, NH_4^+, K^+, Na^+, Ca^{2+}, and Mg^{2+}) were quantified by an ion chromatograph (940 Professional IC Vario, Metrohm) following procedures described by Cai et al. (2020).

The aerosol liquid water content (ALWC) and acidity (pH) were calculated using the ISORROPIA-II thermodynamic model. ISORROPIA-II was run in forward mode, assuming the particles were in a "metastable" state. The input parameters included environmental relative humidity (RH), temperature (T), and the inorganic components of the particle phase (SO_4^{2-}, NO_3^-, Cl^-, NH_4^+, K^+, Na^+, Ca^{2+}, and Mg^{2+}) (Guo et al., 2015; Hennigan et al., 2015; Song et al., 2018b; Weber et al., 2016). In this study, no gaseous NH_3 data were available at the sampling sites. Wang et al. (2020b) showed that the estimated aerosol pH values, when NH_3(g) was not input into the model, had an average deviation of −0.97 pH units. Earlier studies also indicated that when NH_3(g) was not included in the model, a system bias of −1 pH unit needed to be considered when calculating aerosol pH values (Guo et al., 2015). Therefore, due to the lack of NH_3(g) data, a correction of 1 pH unit was applied when calculating aerosol pH values for both summer and winter.

2.3 Data processing and statistical analysis

Raw data were acquired using Xcalibur software (V2.2; Thermo Scientific). The HPLC-HRMS data were processed with MZmine-2.33 software (http://mzmine.github.io) to obtain the *m/z* ratios, formulas, retention times, and peak

https://doi.org/10.5194/egusphere-2026-2472
Preprint. Discussion started: 13 May 2026

areas of detected organic compounds (Cai et al., 2024; Hu et al., 2016; Wang et al., 2017). The molecular formula assignment was mainly based on detected *m/z* values with a mass tolerance of ± 2 ppm. The compounds assigned as $C_{1-40}H_{1-100}O_{1-20}N_{0-4}S_{0-2}$ with s = 1 or 2 will be collectively referred to as organosulfur compounds, including CHOS (n = 0) and CHONS (n = 1 or 2).

For chemical formula $C_cH_hO_oN_nS_s$, the double bond equivalent (DBE) value, representing the degree of unsaturation, can be calculated by Eq. (1):

$$DBE = (2c + 2 + n - h)/2 \quad (1)$$

The aromaticity equivalent (X_C) was introduced by Yassine et al. (2014) for the identification and characterization of monocyclic and polycyclic aromatic compounds. The Xc for compounds containing only carbon, hydrogen, nitrogen, oxygen, and sulfur can be calculated following Eq. (2):

$$Xc = \frac{3[DBE - (i \times o + j \times s)] - 2}{DBE - (i \times o + j \times s)} \quad (2)$$

where i and j correspond to the fractions of oxygen and sulfur atoms involved in the π-bond structures of a compound, respectively. Here, $i = j = 0.5$ was applied for the calculation of X_C values of compounds detected in ESI−, as carboxylic compounds with p = q = 0.5 are preferably ionized in negative mode (Tong et al., 2016; Wang et al., 2017). If DBE ≤ $i \times o + j \times s$, then X_C was defined as zero. The ranges of 2.50 ≤ Xc < 2.71, 2.71 ≤Xc < 2.80, 2.80 ≤Xc < 2.83, and 2.83 ≤Xc are proposed as unambiguous minimum criteria for the presence of mono-, di-, tri-, and polycyclic aromatics, respectively (Yassine et al., 2014).

Given the large number of detected OrgSs, it is impractical to evaluate the ionization efficiencies of each compound. In this study, qualitatively comparing the variation trends of different compounds detected by HR-MS is a commonly used and valid approach for characterizing the overall molecular composition of OA across different sites or seasons (Cai et al., 2020; Wang et al., 2024b; Zhang et al., 2024). Accordingly, despite the potential influence of matrix effects, analyzing and comparing the number or signal intensity percentages of different OrgS categories can, to some extent, reflect the variability in the molecular composition of OrgSs under varying atmospheric conditions. To further assess the impact of matrix effects in different samples, we spiked all samples with 200 ppb of D_{17}-Octyl sulfate as an internal standard (IS). The IS intensity exhibited minimal variability across different samples, indicating that matrix effects on ionization efficiency can be considered negligible. The relative abundance of each compound refers to its chromatographic peak area, and all detected abundances were blank-corrected. To facilitate more accurate comparisons, the relative abundance of each OrgS compound was defined as the ratio of its absolute abundance

https://doi.org/10.5194/egusphere-2026-2472
Preprint. Discussion started: 13 May 2026

to that of IS (set as 100%) within the same sample.

To evaluate the associations between environmental variables and OrgSs in suburban summer, urban summer, and urban winter, nonmetric multidimensional scaling (NMDS) analysis was conducted based on Bray–Curtis distances in R using the vegan package (Jiang et al., 2022). For all three sample sets, the OrgS compounds were dimensionally reduced to two components (NMDS1 and NMDS2), and all stress values were less than 0.15. The selected environmental parameters, including meteorological parameters (T and RH), gaseous pollutants (NO_2, CO, SO_2, O_3, and NO), chemical tracers (EC, K^+, and Cl^-), inorganic nitrogen and sulfur species (SO_4^{2-}, NO_3^- , and NH_4^+) as well as ALWC and pH, were fitted onto the ordination plot to evaluate the key environmental drivers influencing the molecular distributions of OrgSs. The significance (*p*-values) of the correlations between the environmental parameters and the NMDS dimensions was assessed using 999 permutations. Only the factors significantly correlated with the NMDS dimensions were reserved and could be considered as the possible drivers associated with molecular distribution. Score and loading plots were constructed according to NMDS variables from each OrgSs compound (gray triangles and circles). The potential driving factors associated with the molecular distribution of OrgSs were indicated by arrows, with their direction and angle representing the relationship between the variables and each dimension. Spearman correlation between the sum-normalized peak areas of individual molecules and some important environmental variables and chemical tracers was performed in R, and then VK diagrams were plotted for each variable based on the Spearman correlation coefficients (Kellerman et al., 2014). Molecules found in at least four samples were adopted for correlation analysis. A false discovery rate-adjusted *p*-value was applied to avoid errors arising from using a large dataset.

3 Results and discussion

3.1 Molecular Characteristics of OrgSs

By using UHPLC-Orbitrap MS analysis, a total of 1964, 1914, and 2689 organosulfur formulas were detected in suburban summer, urban summer, and urban winter aerosol samples, respectively. The intensity and number of detected OrgSs were significantly higher in winter than in summer, which aligns with the seasonal variations in $PM_{2.5}$ and organic matter mass concentrations (Table S1). The elevated number of OrgS species detected in urban winter further indicates a highly complex molecular diversity during the cold season. The identified OrgSs can be classified into six categories: $CHOS_1$, $CHOS_2$, $CHON_1S_1$, $CHON_1S_2$, $CHON_2S_1$, and $CHON_2S_2$. $CHOS_1$

https://doi.org/10.5194/egusphere-2026-2472
Preprint. Discussion started: 13 May 2026

and $CHON_{1-2}S_1$ account for ~88% of the molecular number and ~96% of the total intensity of OrgSs (Table S2), suggesting their dominant roles in OrgS composition. Notably, the intensity contribution of $CHOS_1$ in suburban summer was lower than those in urban summer and winter, whereas $CHON_{1-2}S_1$ showed an opposite trend. This disparity underscores the distinct influences of geographical location and seasonality on OrgS composition, as discussed in detail below. Furthermore, as many as 79%—92% of OrgS species contained enough oxygen atoms to enable the assignment of $-OSO_3H$ and $-ONO_2$ groups (e.g., $(4s + 3n)/o \leq 1$) in their formulas, suggesting that they were potential OSs or nitrooxy-OSs (NOSs), which is consistent with previous studies (Cai et al., 2020; Wang et al., 2016). The assignments of most OSs were further conducted based on their sulfur-containing fragment ions (e.g., $SO_3^{\bullet-}$ *m/z* 79.96, HSO_3^- *m/z* 80.92, and HSO_4^- *m/z* 96.96) in collisional activation mass spectrometry (Hettiyadura et al., 2015; Riva et al., 2016a).

3.1.1 CHOS species

CHOS species predominated in both suburban and urban samples, accounting for 65% − 77% of the total OrgS intensity (Table S2). The majority (83% − 88%) of CHOS formulas were assigned with $4s/o \leq 1$, suggesting that these compounds are potential OSs (Lin et al., 2012b). Clear seasonal differences were observed in their molecular characteristics. In urban samples, CHOS species in summer exhibited higher O/C_w and H/C_w ratios ($O/C_w = 0.53 \pm 0.11$, $H/C_w = 1.81 \pm 0.04$) than those in winter ($O/C_w = 0.45 \pm 0.06$, $H/C_w = 1.62 \pm 0.03$), whereas the average DBE_w of wintertime CHOS compounds (2.56 ± 0.47) exceeded that in summer (2.18 ± 0.44). These results indicate that wintertime CHOS species were characterized by the lower oxidation state and higher unsaturation degree and aromaticity, likely associated with intensified anthropogenic emissions in winter and enhanced photochemical processing in summer. The enhanced anthropogenic influence in winter can be further supported by the aromaticity equivalent (Xc), a parameter determining the presence of monoaromatics ($Xc \geq 2.50$) and polyaromatics ($Xc \geq 2.71$) (Yassine et al., 2014). As depicted in Figure 1b,c,f, the intensity fraction of CHOS compounds with $Xc \geq 2.5$ was greater in winter (18 ± 8%) than in urban summer (10 ± 5%). Aromatic CHOS compounds were dominated by phenyl OrgSs with $2.50 \leq Xc < 2.71$, accounting for 70 ± 14% and 73 ± 9% of the total aromatic CHOS peak intensity in summer and winter, respectively, which possibly suggests significant influences from primary anthropogenic emissions (Cui et al., 2019; Ma et al., 2014; Song et al., 2018a). Furthermore, the intensity fraction of polyaromatic CHOS compounds ($Xc \geq 2.71$) increased from summer (3 ± 2% in urban) to winter (5 ± 2%), suggesting enhanced combustion emission during the cold

https://doi.org/10.5194/egusphere-2026-2472
Preprint. Discussion started: 13 May 2026

season. This interpretation is consistent with the nearly twofold higher concentrations of combustion-related tracers (e.g., EC and CO) in winter than in summer. In contrast, higher temperatures and O_3 levels in summer likely facilitated stronger biogenic VOC emissions and more intense photochemical oxidation. All of those highlight seasonal differences in emission sources and secondary transformation processes of CHOS species in urban Shanghai.

Compared with urban summer, CHOS species in suburban summer exhibited slightly higher average O/C_w (0.58 ± 0.14) and H/C_w (1.88 ± 0.06) ratios, and a lower DBE_w value (2.06 ± 0.46), indicating a relatively higher degree of oxygenation and saturation in suburban CHOS species. Correspondingly, the intensity fractions of phenyl CHOS and polyaromatic CHOS in suburban summer were 7% ± 5% and 2% ± 1%, respectively, both slightly lower than those in urban summer. This spatial disparity is consistent with the weaker anthropogenic influence at the suburban site, where the average concentrations of EC and CO were approximately half of those observed at the urban site (Table S1). Conversely, the higher average O_3 level at the suburban site suggests stronger oxidative processing. These results imply that suburban CHOS composition was more strongly influenced by the oxidation of biogenic VOCs under summer conditions. Regionally, the H/C_w ratios of CHOS in this study were comparable to or exceeded those reported for ambient aerosols from diverse locations worldwide (Table S3) (Jiang et al., 2022; Lin et al., 2012a; Ning et al., 2025; O'Brien et al., 2014; Rincón et al., 2012; Wang et al., 2024a; Willoughby et al., 2014), suggesting that the OrgSs in Shanghai are relatively enriched with saturated structures. However, the O/C_w ratios of CHOS compounds identified in this study were slightly higher than that reported for $PM_{2.5}$ in Anshan (0.45) (Ning et al., 2025) and comparable to values measured in the Pearl River Delta (0.52 ± 0.07) (Jiang et al., 2022), but markedly lower than those reported for aerosols from California (0.82 − 0.93) and polluted organic aerosols from Mainz (0.78 − 1.44) and Chinese (1.17 − 1.48) cities (O'Brien et al., 2014; Wang et al., 2021a; Wang et al., 2018a; Wang et al., 2019). Such regional discrepancies suggest that CHOS in Shanghai is likely driven by emissions from different sources and subsequently undergoes complex atmospheric oxidation processes. This also implies that, owing to pronounced spatiotemporal heterogeneity, CHOS in Shanghai may exhibit a distinct molecular composition relative to other regions, highlighting the need for further investigations into OrgS sources and their molecular-level distributions.

The most abundant class of CHOS species identified in all samples had 4 − 7 O atoms, with S_1O_5 being the most prevalent (Fig. 1d and S1a). This characteristic was most evident in the urban winter samples. The elevated oxygen content implies the presence of additional oxidized functional groups, such as hydroxyl and carbonyl. As

https://doi.org/10.5194/egusphere-2026-2472
Preprint. Discussion started: 13 May 2026

shown in Figures 1a–c, the main distribution of CHOS compounds falls within a DBE range of 1 to 10 and a carbon number range of 2 to 22. Based on established DBE classifications (Jiang et al., 2022; Lin et al., 2012b), the detected CHOS species were tentatively classified into three categories: saturated aliphatic-derived species (DBE ≤ 1; 51 ± 10%), biogenic-derived species (DBE=2/3; 23 ± 12%), and aromatic-derived species (DBE ≥ 4; 26 ± 15%), collectively accounting for the total intensity of assigned CHOS compounds (Fig. 1e). CHOS compounds with DBE ≤ 3 predominantly contained 8 to 22 carbon atoms, accounting for 59 ± 13% of the total CHOS intensity. The C_8–C_{22} compounds are likely associated with the oxidation products of monoterpenes (C_{10}) and sesquiterpenes (C_{15}), as well as dimeric and trimeric BVOC oxidation products (Daellenbach et al., 2019; Kourtchev et al., 2016). However, anthropogenic sources have also been proposed for C_8–C_{22} CHOS compounds, including the photooxidation of long-chain alkanes from vehicle emissions (Riva et al., 2016a; Tao et al., 2014) and heterogeneous reaction between SO_2 and unsaturated fatty acids in ambient particles (Shang et al., 2016; Zhu et al., 2019). For example, $C_{10}H_{18}O_6S$ and $C_{10}H_{18}O_7S$ could be formed via photooxidation of both biogenic (α-pinene) and anthropogenic (cyclodecane) precursors (Riva et al., 2016a; Surratt et al., 2008). These findings underscore the challenge of unambiguous source apportionment based solely on molecular formula. In addition to the dominant C_8–C_{22} compounds, low molecular weight CHOS compounds (C_2–C_7) with DBE ≤ 3 were also observed, which are likely isoprene derivatives or fragmentation products generated during atmospheric oxidation processes (Hatch et al., 2011; Riva et al., 2016b). High molecular weight compounds (C > 22) contributed minimally to the total CHOS signal. Among the CHOS compounds, five species (e.g., $C_9H_{16}O_7S$, $C_{10}H_{20}O_5S$, $C_{12}H_{26}O_4S$, $C_{14}H_{28}O_5S$, and $C_{16}H_{34}O_5S$) were identified as the dominant components in OA. $C_9H_{16}O_7S$ has been proposed to be mainly derived from the photooxidation of limonene/limonaketone in the presence of acidified sulfate seed aerosol (Surratt et al., 2008). The remaining four species, characterized by saturated aliphatic structures with DBE ≤ 1, suggest that their formation likely involves atmospheric oxidation and subsequent sulfation of unsaturated fatty acids or long-chain alkanes (Riva et al., 2016a; Shang et al., 2016; Tao et al., 2014).

3.1.2 CHONS species

Although CHONS species contributed less to the total OrgS intensity than CHOS species, their nitrogen-containing molecular structures suggest their potential importance in the atmospheric nitrogen cycle, acting as important reservoirs for organic nitrogen. As shown in Table S2, a total of 895, 787, and 1277 CHONS molecular

https://doi.org/10.5194/egusphere-2026-2472
Preprint. Discussion started: 13 May 2026

formulas were assigned in suburban summer, urban summer, and urban winter aerosol samples, respectively, accounting for 35%, 23% and 26% of the total intensity of OrgSs, respectively, which underscores that CHONS species were an important component of particulate OrgSs in suburban atmospheric environments. In winter, the average MW_w, O/C_w, and DBE_w values of CHONS compounds were 322 ± 9.08, 0.65 ± 0.17, and 6.02 ± 2.60, respectively (Table S2), which were higher than those of CHOS compounds (MW_w: 285 ± 15.4, O/C_w: 0.45 ± 0.06, DBE_w: 2.56 ± 0.47), probably due to the presence of additional nitrate ($-ONO_2$) functional groups (Wang et al., 2019). This trend was also observed in suburban and urban summer samples. Similar to CHOS species, the DBE_w values of CHONS species in urban winter were 1.23 and 1.41 times higher than those observed in urban and suburban summer, respectively, while their average O/C_w values were lower in urban winter. Moreover, CHONS species in suburban summer were characterized by the highest H/C_w and O/C_w ratios, and the lowest DBE_w and Xc_w values. These results indicate that the molecular distributions of CHONS species were likely shaped by seasonal and spatial differences in emission sources and atmospheric oxidative capacity. Additionally, the results from the comparison between the average H/C_w and O/C_w ratios of CHONS compounds and those reported previously were consistent with those observed for CHOS species (Table S4). For example, the O/C_w ratios of CHONS compounds here were lower than those reported in six Chinese megacities (Wang et al., 2024a).

CHONS species were primarily dominated by those with more than 6 oxygen atoms (45−75% in total) on individual days (Fig. S2a). In summer, the number of CHONS species containing $O \geq 10$ was substantially higher than in winter, likely attributable to enhanced photochemical oxidation processes during the summer (Cai et al., 2020; Fan et al., 2022b). Furthermore, the suburban site exhibited a notably higher number of CHONS species with $O \geq 10$ compared to the urban site during the summer. This spatial discrepancy may be associated with reduced NO titration effects, higher O_3 exposure (Table S1), and more abundant biogenic precursor emissions in the suburban atmosphere (Surratt et al., 2008; Wang et al., 2020b). The identified CHONS compounds spanned $N_1S_1O_1$ – $N_1S_1O_{12}$ and $N_2S_1O_1$ – $N_2S_1O_{12}$, with $N_1S_1O_7$ class exhibiting the highest relative abundance. Their DBE and carbon number distributions closely resembled those of CHOS species (Fig. 2a−c). Although CHONS compounds containing two N atoms were also identified, their relatively low intensity suggests a minor contribution compared to those with one N atom. The average DBE_w of $CHON_2S_1$ species was approximately 3 − 4 times higher than that of $CHON_1S_1$ compounds at both sites, implying that $CHON_2S_1$ probably contains numerous aromatic NOSs, whereas $CHON_1S_1$ species are predominantly composed of NOSs featuring long

https://doi.org/10.5194/egusphere-2026-2472
Preprint. Discussion started: 13 May 2026

aliphatic carbon chains with low degrees of oxidation and unsaturation (Fig. 2a–c and Table S2). Based on the (DBE − N) value, which serves as a more reliable indicator of aromaticity (Lin et al., 2012b), CHONS compounds were dominated by olefinic species (DBE − N = 2/3), followed by saturated aliphatic (DBE − N ≤ 1) and aromatic (DBE − N ≥ 4) compounds. Notably, the most abundant saturated aliphatic and olefinic CHONS species fell within the C8 − C12 range with O ≥ 7 (Fig. 2e). $C_{10}H_{17}NO_7S$ (*m/z* = 294.0653, DBE=3; Fig. 2c and S3) was the most abundant CHONS formulas across most samples. This species has been proven to be formed via atmospheric oxidation of α-pinene (Surratt et al., 2008). Nevertheless, recent evidence has confirmed its presence in coal combustion-generated aerosols (Song et al., 2018a), suggesting this compound likely has mixed sources in polluted environments. The tentatively assigned NOSs contributed comparably to the total number of CHONS species across both sites, accounting for 56% − 60%, which was notably lower than that of OSs in CHOS species (83% − 88%) (Table S2). The intensity fraction of NOSs in CHONS species was higher at the urban site (89 ± 10%) than at the suburban site (73 ± 10%) during summer. This disparity can plausibly be attributed to elevated NO_x levels in the urban environment (Table S1), which promote NOS formation via reactions with CHOS species or other organic precursors in the presence of acidic aerosols (Fan et al., 2022a; Hamilton et al., 2021; Surratt et al., 2008). This result also revealed that other N- or S-containing heteroatom compounds in CHONS species, such as those derived from the oxidation of pyrrole and thiophene (Jiang et al., 2019), contributed a smaller intensity fraction at the urban site (11 ± 2%) than at the suburban site (27 ± 4%).

3.2 Potential precursor assignment of organosulfur species

The detected OSs were classified into four groups based on their potential precursors, including BVOC-derived OSs (e.g., isoprene/monoterpene/sesquiterpene-derived OSs and other BVOC-derived OSs from the precursors of green leaf volatiles), anthropogenic VOCs (AVOC)-derived OSs from the precursors of PAHs and anthropogenically emitted alkanes, multiple-sources-derived OSs, and OSs with unidentified precursors. The potential precursors of multiple-sources-derived OSs include carbonyl compounds (e.g., glyoxal and glycolaldehyde), unsaturated fatty acids, and long-chain alkenes emitted from biogenic and/or anthropogenic sources (Fu et al., 2008; Passananti et al., 2016; Shang et al., 2016). The precursor assignment of OSs was performed by matching the measured OS molecular formulas to the published OSs whose precursors have been verified. This approach has been widely used because its feasibility relies on the high mass resolution of HR-MS, which enables reliable mass peak detection and the assignment of formulas within a narrow mass tolerance (Cai et

https://doi.org/10.5194/egusphere-2026-2472
Preprint. Discussion started: 13 May 2026

al., 2020; Wang et al., 2019; Yang et al., 2023). Details of these OS formulas with the determined precursors are listed in Tables S5−S9.

Figure 3e shows the intensity distribution of OSs derived from various precursors among the three campaigns. A total of 270 OS molecular formulas could be assigned to potential precursors, accounting for approximately 70% of the total CHOS intensity. Among them, BVOC-derived OSs contributed 32 ± 13% in suburban summer, 30 ± 12% in urban summer, and 28 ± 6.7% in urban winter, whereas AVOC-derived OSs accounted for 16 ± 4.6%, 18 ± 4.7%, and 20 ± 2.4%, respectively. These results are consistent with the molecular signatures discussed above, suggesting relatively stronger biogenic contributions in suburban and urban summer, but enhanced anthropogenic influences in urban winter. Monoterpene-derived OSs constituted the dominant fraction of BVOC-derived OSs. Several highly abundant formulas of monoterpene-derived OSs, including $C_9H_{16}O_6S$ (*m/z* 251.0595), $C_{10}H_{18}O_5S$ (*m/z* 249.0802), and $C_9H_{16}O_7S$ (*m/z* 267.0544), and $C_{10}H_{18}O_7S$ (*m/z* 281.0701), have been frequently reported in ambient aerosols and are commonly attributed to acid-catalyzed reactions of monoterpene oxidation products (Bruggemann et al., 2020; Surratt et al., 2008; Wang et al., 2020b). By contrast, isoprene-derived OSs contributed a much smaller fraction to the total CHOS intensity than monoterpene-derived OSs.

For identified AVOC-derived OSs, aromatic-derived OSs contributed only minor fractions to the total CHOS intensity in suburban summer (1.3 ± 0.4%), urban summer (1.5 ± 0.6%), and urban winter samples (1.9 ± 0.7%), whereas long-chain alkane-derived OSs accounted for much larger fractions (15 ± 4.5%, 17 ± 4.6%, and 18 ± 2.4%, respectively). Polycyclic aromatic hydrocarbons have been recognized as important precursors of aromatic OSs based on laboratory and field evidence (Kundu et al., 2013; Riva et al., 2015). Aromatic OSs with benzyl and polycyclic aromatic carbon backbones, such as $C_6H_6O_4S$, $C_7H_6O_4S$, $C_7H_8O_4S$, $C_8H_8O_4S$, and $C_9H_{12}O_5S$ derived from the photooxidation of naphthalene and 2-methylnaphthalene (Riva et al., 2015), have been widely observed in urban and semi-rural fine aerosols worldwide (Bruggemann et al., 2020; Jiang et al., 2022; Wang et al., 2019; Yang et al., 2023), and were also detected in our samples. Nevertheless, despite their frequent occurrence, only a few aromatic OSs with relatively low intensity could currently be unambiguously classified. In contrast, aromatic CHOS species with Xc ≥ 2.5 accounted for 16 ± 3.8% and 19 ± 2.9% of total CHOS species by number in suburban and urban summer, respectively, and increased to 22 ± 3.4% in urban winter, suggesting enhanced anthropogenic emissions in winter. The intensity fractions of aromatic CHOS in Shanghai (7% −18%) were comparable to those reported for Guangzhou (9%−20 %) (Jiang et al., 2022), further underscoring a non-negligible influence of anthropogenic emissions on the molecular

https://doi.org/10.5194/egusphere-2026-2472
Preprint. Discussion started: 13 May 2026

composition of atmospheric OrgSs in Chinese megacities. In addition, multiple-source OSs showed a slight increase in their contribution to total CHOS intensity from suburban summer (22 ± 7.2%) to urban summer (23 ± 6.8%) and further to urban winter (27 ± 6.9%), probably hinting a stronger influence of anthropogenic emissions on their sources and formation processes.

The precursors for 28 ± 15% of OS molecular formulas cannot yet be confidently recognized. Among these, subgroup B, defined as organosulfates with $C > 8$, $DBE < 3$, and $3 < O < 7$ for CHOS, contributed 6.7 ± 3.3%, 16 ± 8.3%, and 8.7 ± 2.5% to the total CHOS intensity in suburban summer, urban summer, and urban winter, respectively. Subgroup B is characterized by a high molecular weight, long alkyl chains, and a low degree of unsaturation and oxidation. Tao et al. (2014) speculated that the precursors of subgroup B could be long-chain alkanes from traffic emissions. Long-chain alkanes can undergo rapid photooxidation under typical urban conditions (Lim & Ziemann, 2009; Yee et al., 2013), yielding hydroxylated or carbonylated intermediates that were further esterified to form alkyl OSs in acidic aerosol. Riva et al. (2016a), through smog-chamber photooxidation experiments of long-chain alkanes, revealed that alkane-derived OSs can also form via gaseous epoxide precursors with subsequent acid-catalyzed reactive uptake onto sulfate aerosols and/or heterogeneous reactions of hydroperoxides (Fig. 6d). Moreover, the formation of OSs from heterogeneous reactions of gaseous SO_2 with unsaturated fatty acids (USFA) was also important for these highly saturated OSs (Shang et al., 2016; Zhu et al., 2019). Large amounts of USFA have been observed in high-temperature cooking emissions, especially Chinese-style cooking with more frying, which is among the important emission sources in urban areas (Zhao et al., 2015; Zhu et al., 2019). Accordingly, subgroup B contributed more to total CHOS at the urban site (16 ± 8.3%) than at the suburban site (6.7 ± 3.3%) during the summer, indicating a greater influence of urban hydrocarbon emissions. Moreover, the intensity fraction of subgroup B showed positive correlations with RH (Fig. S3a), suggesting that humidity-driven heterogeneous or multiphase processing may facilitate the formation of these long-chain OSs. Although aromatic VOCs have been widely studied as drivers of particulate air pollution in densely populated regions like Shanghai (Gao et al., 2019; Han et al., 2023a), our results suggest that long-chain hydrocarbons and their corresponding OS products also play an important role in the formation of particulate organosulfurs in urban atmospheres.

In contrast to the relatively well-established precursor assignments for CHOS compounds, only a limited number of CHONS species could be linked to specific precursors (Tables S5−S9). Therefore, we further evaluated the potential precursor origins of CHONS species based on their Van Krevelen distributions, the precursor-

https://doi.org/10.5194/egusphere-2026-2472
Preprint. Discussion started: 13 May 2026

based classification of NOSs, and molecular fingerprints from representative source samples. As shown in Figure 4a−c, CHONS compounds, particularly NOSs, were predominantly distributed in the unsaturated aliphatic region (H/C ≈ 1.5−2.0，(O−3S−2N)/C ≈ 0.1−0.6), suggesting that their precursors are mainly derived from the oxidation products of BVOCs, such as isoprene and monoterpenes (Hamilton et al., 2021; Lin et al., 2012b; Surratt et al., 2008), with additional contributions from traffic-related alkenes and long-chain hydrocarbon oxidation intermediates (Riva et al., 2016a; Tao et al., 2014). The distributions of suburban and urban samples in summer were broadly similar, indicating comparable dominant precursors and formation mechanisms. In contrast, urban winter samples exhibited a more constrained distribution toward lower (O−3S−2N)/C values, consistent with a stronger influence of NO_3-initiated nighttime oxidation under high NO_x, low temperature, and reduced photochemical activity (Brown & Stutz, 2012; Hamilton et al., 2021). Figure 5e shows that seasonal variability was more influential than spatial differences in shaping NOS composition. Monoterpene-derived NOSs predominated in most samples (11%−78%), underscoring monoterpenes as important precursors of NOSs, which aligns with previous studies (Lin et al., 2012b; Surratt et al., 2008). In contrast, the relative contribution of isoprene-derived NOSs decreased markedly in urban winter, likely due to reduced isoprene emissions under low-temperature conditions (Guenther et al., 2012; Li et al., 2011). Furthermore, monoterpene-derived NOSs exhibited noticeable diurnal variability, especially in summer, with generally higher contributions at night (Fig. 4e and S4), which is consistent with an important role of nighttime NO_3-initiated oxidation in NOS formation (Brown & Stutz, 2012; Ng et al., 2017).

To further constrain the possible precursor origins of CHONS, we compared their molecular characteristics with those reported for representative source samples in previous studies, including coal combustion organic aerosols (CCOAs), biomass burning organic aerosols (BBOAs), vehicle emissions, tunnel aerosols, and emissions from nonroad excavators and ships (Cui et al., 2019; Tang et al., 2020a) . As shown in Figure 4a−d, substantial overlap in CHONS species was observed between our field samples and previously reported source samples, particularly in the high H/C region. However, ambient samples extended toward more oxidized regions, indicating that CHONS species are predominantly formed via secondary processes rather than direct primary emissions. The most abundant CHONS species in Shanghai were dominated by unsaturated aliphatic compounds (Fig. 4a−d), whose overall characteristics more closely resembled those of tunnel aerosol samples that had likely undergone atmospheric aging processes. By contrast, CHONS compounds in fresh vehicle emissions were abundant in aromatics, with 59% of the identified CHONS species

https://doi.org/10.5194/egusphere-2026-2472
Preprint. Discussion started: 13 May 2026

showing Xc ≥ 2.50 (Table S11). Likewise, a large number of aromatic and highly unsaturated CHONS species were detected in both BBOAs and CCOAs, but their molecular characteristics differed substantially from the dominant CHONS components observed in Shanghai. Notably, although approximately 36%, 40%, and 44% of CHONS species by number could be classified as aromatic organosulfur compounds in suburban summer, urban summer, and urban winter, respectively, most of these species exhibited relatively low abundances (Fig. 4a–d and Table S11). Thus, although combustion sources can directly emit a large variety of CHONS compounds, the low-oxidation and aromatic CHONS species that dominate the source samples contributed only weakly to the MS intensity of the ambient CHONS pool observed here. These results suggest that the CHONS in Shanghai may be less influenced by primary emissions and more likely driven by secondary formation processes, such as secondary formation via combustion-emitted precursors. Similar features were also observed in the comparison between CHOS species detected in our field samples and source samples (Fig. 3 and Table S10).

Taken together, the precursor assignment and source comparison highlight the important role of secondary formation from both biogenic and anthropogenic precursors in shaping the molecular composition of particulate OrgSs in Shanghai. Given that isoprene- and monoterpene-derived OSs and NOSs are representative BVOC-derived species and are sensitive to variations in precursor emissions, oxidant regimes, NO_x/NO_3 chemistry, and sulfate-related multiphase processing, their spatial, seasonal, and diurnal variability was further examined.

3.3 Spatiotemporal variability of isoprene/monoterpene-derived OSs and NOSs

During summer, isoprene/monoterpene-derived OSs at both suburban and urban sites exhibited distinct diurnal variation, with significantly higher relative abundance during the day than at night ($p < 0.05$; Fig. 5a,b). This pattern highlights the dominance of daytime photochemical processes, likely driven by enhanced biogenic emissions under high temperatures and intense solar radiation, followed by •OH-initiated oxidation (Surratt et al., 2010; Xu et al., 2015). In contrast, no significant diurnal variation was observed in winter urban samples ($p > 0.05$), suggesting that the formation of these OS species in winter was less controlled by a single photochemical pathway and more influenced by multiple pathways under low-temperature, weak-radiation, and high-NO_x conditions. Notably, isoprene-derived OSs showed only weak seasonal differences, whereas monoterpene-derived OSs were more abundant in winter than in summer (Fig. 5a,b). This appears to suggest that enhanced nighttime and/or heterogeneous production in winter may partially compensate for the decline in

https://doi.org/10.5194/egusphere-2026-2472
Preprint. Discussion started: 13 May 2026

photochemical efficiency. Recent studies suggested that OSs could also be formed through heterogeneous or multiphase reactions between SO_2 and monoterpene-derived SOA or unsaturated fatty acids in the particle phase (Fig. 6b) (Yao et al., 2019; Zhu et al., 2019). Since SO_2 levels during our winter campaign was 1.6−1.8 times higher than those during the summer campaigns (Table S1), such formation pathways involving SO_2 likely led to the higher abundance of monoterpene-derived OSs in winter. Such compensation may also be aided by additional inputs of isoprene and monoterpenes from anthropogenic activities, such as biomass burning, which could help sustain OS formation under cold conditions (Akagi et al., 2011; Gilman et al., 2015; Yang et al., 2025). Overall, these results suggest that photochemistry was the dominant driver of isoprene/monoterpene-derived OS formation in summer, whereas wintertime formation was governed by a more complex, multi-pathway regime involving nocturnal NO_3• chemistry and heterogeneous or multiphase processes.

The diurnal patterns of monoterpene/isoprene-derived NOSs differed markedly from those of OSs. The day–night variations of isoprene-derived NOSs were not obvious across the three field campaigns (Fig. 5c), suggesting that their formation may be jointly influenced by daytime •OH oxidation and nighttime NO_3• oxidation. In contrast, monoterpene-derived NOSs exhibited obvious nighttime enhancements ($p < 0.05$; Fig. 5d), with significantly higher relative abundances at night than during the day in both suburban and urban summer samples ($p < 0.01$). This trend underscores that •NO_3-initiated nighttime oxidation is likely an important pathway for their formation (Fig. 6e), consistent with previous field and laboratory studies highlighting the important role of NO_3• oxidation of monoterpenes in NOS formation (Hamilton et al., 2021; Surratt et al., 2008; Yang et al., 2023). Elevated nighttime NO_x levels likely further favored monoterpene-NOS formation via nighttime NO_3• oxidation (Table S1). Moreover, the lower daytime relative abundance of monoterpene-derived NOSs could be exacerbated by daytime photolysis and decomposition processes (He et al., 2011; Wang et al., 2023). Spatial and seasonal variations of monoterpene-derived NOSs further highlight these drivers (Fig. 5d and S4). In summer, monoterpene-derived NOSs were more abundant in suburban than in urban samples, likely reflecting a stronger biogenic influence and the greater importance of monoterpene precursors at the suburban site in the YRD (Ma et al., 2022; Wang et al., 2020a). Notably, their overall relative abundance in urban samples was higher in winter than that in summer, suggesting that a more favorable oxidation environment under high-NO_x conditions may promote the production efficiency of monoterpene-derived NOSs, partly compensating for the typically lower biogenic monoterpene emissions in winter (Wang et al., 2020b). Additionally, previous studies have shown that monoterpenes can also be

https://doi.org/10.5194/egusphere-2026-2472
Preprint. Discussion started: 13 May 2026

emitted from biomass burning, besides their well-known biogenic emission (Akagi et al., 2011; Gilman et al., 2015), which may further contribute to the accumulation of monoterpene-derived NOSs during the cold season.

3.4 Formation Pathways of OrgSs and the influencing factors

Atmosphere OrgSs in Shanghai originate from diverse sources, with secondary formation serving as the dominant contributor. Despite the identification of multiple reaction pathways for OS formation, their formation mechanisms in the real atmosphere remain incompletely understood. Among the known pathways, the acid-catalyzed ring-opening reaction of epoxides derived from the oxidation of VOCs is widely recognized as a kinetically feasible and key mechanism for the atmospheric formation of OSs (Fig. 6a) (Bruggemann et al., 2020; Cai et al., 2020). For instance, previous studies have demonstrated that high concentrations of isoprene-derived OSs observed in Beijing and Guangzhou were mainly produced through the acid-catalyzed ring-opening of isoprene epoxydiol intermediates (Jiang et al., 2022; Wang et al., 2018b). Furthermore, NOSs can be formed via the nighttime NO_3-initiated oxidation of monoterpenes on acidic sulfate seed particles (Ng et al., 2017; Surratt et al., 2008). The formation and molecular distribution of OS and NOS products are generally governed by multiple environmental factors, including precursor abundance (e.g., organic precursors and anthropogenic pollutants such as NO_x and SO_2), aerosol acidity, RH, and oxidant levels. To disentangle how these complex variables drive the molecular distribution of OrgSs across different spatiotemporal settings (suburban summer, urban summer, and urban winter), NMDS analysis of OrgSs was conducted (Fig. 7). Overall, samples from different seasons and urban/suburban sites exhibit distinct separation in the two-dimensional ordination space, indicating that the molecular composition of OrgSs is highly sensitive to changes in precursor sources, oxidation conditions, and the particulate-phase reaction environment.

For suburban summer samples, Cl^- was positively correlated with the NMDS1 dimension, whereas tracers indicating combustion emissions (EC and CO), biomass burning (K^+), and secondary inorganic nitrogen species (NO_3^-), were mainly distributed on the negative direction of NMDS1 (Fig. 7a). This suggests that the NMDS1 dimension may reflect the integrated influence of different air mass sources on the molecular composition of OrgSs. It should be noted that Cl^- can originate from both combustion sources (e.g., coal smoldering) and marine aerosols (Wu et al., 2024). Given that the sampling site was situated in a coastal region and that Cl^- exhibits an opposite trend to typical combustion tracers like EC, Cl^- is more likely to represent the influence of marine air masses or sea-salt input. Therefore, the divergent trends of Cl^- and EC along the NMDS1 axis may highlight the distinct impacts of anthropogenic

https://doi.org/10.5194/egusphere-2026-2472
Preprint. Discussion started: 13 May 2026

versus marine sources on the molecular composition of OrgSs in suburban summer. Notably, the suburban summer samples exhibited a pronounced diurnal separation along the NMDS2 dimension. Daytime samples primarily clustered along the positive axis of NMDS2, aligning with T and O_3; conversely, nighttime samples aggregated in the negative direction, consistent with RH and NO_2. These results indicate that the molecular composition of OrgSs during the daytime was more strongly governed by high temperature and photochemical oxidation processes. In summer, elevated daytime temperatures facilitate the emission of volatile organic compounds (VOCs), especially BVOCs, while stronger photochemistry and enhanced O_3 levels further promote the oxidation of VOCs and the subsequent formation of OSs. In contrast, RH and NO_2 emerge as the predominant factors influencing nighttime OrgS composition. On one hand, RH affects OSs formation by influencing the uptake of gaseous precursors like SO_2 by VOCs (Li et al., 2024; Nestorowicz et al., 2018; Ye et al., 2018). On the other hand, NO_2 and its associated nighttime oxidative system (e.g., NO_3 radical) may jointly influence the formation of both OSs and NOSs by modifying the oxidation pathways and product branching of organic precursors, as well as through competition or coupling with heterogeneous processes involving sulfate and acidic particles (Fan et al., 2022b; Hamilton et al., 2021).

For urban summer samples, primary combustion sources related to anthropogenic activities also appeared to play an important role in shaping the molecular composition of OrgSs, whereas the influence of marine air masses was comparatively weak. In contrast to the prominent role of inorganic nitrogen in suburban summer samples, the molecular distribution of OrgSs in urban summer is markedly influenced by SO_4^{2-} (Fig. 7b). This observation aligns with previous studies in Shanghai and other polluted regions, which have highlighted the importance of sulfate-related processes in OS formation (Wang et al., 2018b; Yang et al., 2023). SO_4^{2-} acts not only as a critical reactant but also as a regulator of particle acidity and ALWC, which in turn affects the reactive uptake and heterogeneous conversion efficiency of precursors (Wang et al., 2021b). The distinct influences of different anthropogenic emission species on OrgSs distribution between urban and suburban summer underscore the varying impact of human activities on OS formation across different environments. Nevertheless, the key drivers of the diurnal variation in OrgSs composition were generally consistent between the two sites. Daytime samples cluster with T and O_3 along the positive axis of NMDS2, while nighttime samples aggregate with RH along the negative axis. This result suggests that site type had only a limited influence on the diurnal distribution of OrgSs in summer. The main processes governing the diurnal variability of OrgSs appeared to be broadly similar across the two sites, mainly involving enhanced photochemical

https://doi.org/10.5194/egusphere-2026-2472
Preprint. Discussion started: 13 May 2026

oxidation during the daytime and RH-dependent multiphase processing at night.

For urban winter samples, the NMDS results suggest that the factors influencing the molecular distribution of OrgSs were more complex than those in summer (Fig. 7c). In addition to the impact of primary anthropogenic emissions, inorganic nitrogen and sulfur species emerge as significant drivers, clustering along the negative axis of NMDS1. ALWC is also distributed in the negative NMDS1 direction, suggesting that it was another key parameter associated with the wintertime molecular distribution of OrgSs. ALWC is governed not only by RH, but also by the loading of hygroscopic inorganic components such as NO_3^- and SO_4^{2-}. Under the humid and polluted conditions typical of winter, the accumulation of these species can significantly enhance ALWC and thereby favor aqueous-phase processing (Wang et al., 2021b). For OS formation, elevated ALWC may promote the mass transfer and reactive uptake of SO_2 and oxidized organic intermediates into the particle phase, while it also provides a medium for subsequent aqueous-phase transformations. These results suggest that ALWC is an important particle-phase parameter influencing the formation and molecular composition of organosulfur compounds in winter. Aerosol pH appeared to be another pivotal factor. Lower pH values not only favor the reactive uptake of epoxides and other oxidative intermediates onto acidic sulfate particles, but may also facilitate aqueous-phase esterification via acid-catalyzed mechanisms (Wang et al., 2018b). Therefore, the combination of elevated ALWC and acidic particle conditions likely provided a favorable multiphase reaction environment for the secondary formation and molecular evolution of urban OrgSs in winter. Overall, while the molecular composition of OrgSs in summer was primarily controlled by photochemical oxidation and humidity-driven heterogeneous processes, wintertime OrgSs appeared to be more strongly influenced by the combined effects of enhanced primary emissions, the accumulation of secondary inorganic species, and the synergistic regulation of the particle-phase reaction environment by ALWC and pH.

4. Conclusions and atmospheric implications

This study provides a molecular-level characterization of atmospheric organosulfur compounds (OrgSs) in Shanghai under contrasting atmospheric environments, including suburban summer, urban summer, and urban winter. A total of 1964, 1914, and 2689 OrgS molecular formulas were detected in suburban summer, urban summer, and urban winter aerosol samples, respectively, indicating substantially higher molecular diversity in winter than in summer. OrgSs were dominated by $CHOS_1$ and $CHON_1S_1$ species, which together accounted for most of the detected formulas and

https://doi.org/10.5194/egusphere-2026-2472
Preprint. Discussion started: 13 May 2026

signal intensity. As many as 79%—92% of OrgS species had the elemental composition of $(4s + 3n)/o \leq 1$ in their formulas, suggesting that they were potential OSs or nitrooxy-OSs. The molecular characteristics of both CHOS and CHONS exhibited pronounced seasonal variability. Compared with summer, wintertime OrgSs showed lower O/C ratios but higher DBE values and aromaticity, suggesting a larger contribution from anthropogenic emissions and more unsaturated structures under winter conditions. Although aliphatic structures dominated the OrgS pool overall, the increased abundance of aromatic and polyaromatic species in winter further pointed to enhanced combustion-related influences during the cold season.

Potential precursor analysis showed that BVOC-derived OSs were the largest identified group, followed by OSs derived from anthropogenic VOCs and mixed-source precursors. Monoterpene-derived OSs dominated the biogenic fraction, while the intensity fraction of isoprene-derived OSs increased in summer, especially at the suburban site. In contrast, aromatic and long-chain alkane-derived OSs increased in winter, highlighting a stronger anthropogenic influence. CHONS species showed weaker similarity to primary source profiles and appeared to be more strongly affected by secondary formation, although combustion emissions may still provide important precursors in polluted environments.

The diurnal and seasonal behaviors of isoprene/monoterpene-derived OSs and NOSs revealed distinct controlling mechanisms. In summer, isoprene/monoterpene-derived OSs peaked during the daytime due to photochemical oxidation, whereas monoterpene-derived NOSs were significantly enhanced at night via NO_3-initiated oxidation. The NMDS results further demonstrated that the molecular composition of OrgSs was highly sensitive to seasonal, spatial, and diurnal changes in precursor sources, oxidant levels, and particle-phase reaction conditions. In summer, daytime OrgSs were mainly associated with temperature and O_3, indicating the importance of photochemical oxidation, whereas nighttime composition was more closely linked to RH and NO_2, suggesting a strong role of humidity-driven multiphase processing and nighttime oxidation. The similar day–night separation observed at the suburban and urban sites implies that the dominant mechanisms controlling summer diurnal variability were broadly consistent across different functional zones. In winter, the molecular distribution of OrgSs became more strongly associated with inorganic nitrogen and sulfur species, ALWC, and aerosol acidity, indicating that aqueous-phase and acid-catalyzed processes were more important under polluted winter conditions. Together, these observations suggest that the formation of atmospheric OrgSs in Shanghai is jointly regulated by precursor availability, oxidation pathways, and the physicochemical properties of the particle phase. Overall, this study provides new

https://doi.org/10.5194/egusphere-2026-2472
Preprint. Discussion started: 13 May 2026

molecular-level evidence that improves our understanding of the sources, formation pathways, and environmental controls of atmospheric OrgSs, with implications for interpreting aerosol evolution and for better representing organosulfur chemistry in atmospheric models.

Data availability

The data presented in this work will be uploaded to an open archive prior to publication.

Author contributions

D.C. and X.G. conceived and designed the study. S. Z. and Y.C. carried out the field sampling. D.C., S.R., and Y. F. performed the UHPLC-Orbitrap MS analysis and data processing. X.G. and J. C. acquired funding and undertook project management. D.C. prepared the manuscript with contributions from all co-authors.

Competing interests

The authors declare that they have no conflict of interest.

Acknowledgements

This project is supported by the National Natural Science Foundation of China (42505104; 22336001).

https://doi.org/10.5194/egusphere-2026-2472
Preprint. Discussion started: 13 May 2026

References

Akagi, S. K., Yokelson, R. J., Wiedinmyer, C., Alvarado, M. J., Reid, J. S., Karl, T., et al. (2011). Emission factors for open and domestic biomass burning for use in atmospheric models, *Atmospheric Chemistry and Physics*, 11(9), 4039-4072, https://doi.org/10.5194/acp-11-4039-2011

Brown, S. S., &Stutz, J. (2012). Nighttime radical observations and chemistry, *Chemical Society Reviews*, 41(19), 6405-6447, https://doi.org/10.1039/c2cs35181a

Bruggemann, M., Xu, R., Tilgner, A., Kwong, K. C., Mutzel, A., Poon, H. Y., et al. (2020). Organosulfates in Ambient Aerosol: State of Knowledge and Future Research Directions on Formation, Abundance, Fate, and Importance, *Environ Sci Technol*, 54(7), 3767-3782, https://doi.org/10.1021/acs.est.9b06751

Cai, D., Li, C., Lin, J., Sun, W., Zhang, M., Wang, T., et al. (2024). Comparative study of atmospheric brown carbon at Shanghai and the East China Sea: Molecular characterization and optical properties, *Science of the Total Environment*, 941(173782, https://doi.org/https://doi.org/10.1016/j.scitotenv.2024.173782

Cai, D., Wang, X., Chen, J., &Li, X. (2020). Molecular Characterization of Organosulfates in Highly Polluted Atmosphere Using Ultra-High-Resolution Mass Spectrometry, *Journal of Geophysical Research: Atmospheres*, 125(8), https://doi.org/10.1029/2019jd032253

Cui, M., Li, C., Chen, Y., Zhang, F., Li, J., Jiang, B., et al. (2019). Molecular characterization of polar organic aerosol constituents in off-road engine emissions using Fourier transform ion cyclotron resonance mass spectrometry (FT-ICR MS): implications for source apportionment, *Atmos. Chem. Phys.*, 19(22), 13945-13956, https://doi.org/10.5194/acp-19-13945-2019

Daellenbach, K. R., Kourtchev, I., Vogel, A. L., Bruns, E. A., Jiang, J. H., Petaja, T., et al. (2019). Impact of anthropogenic and biogenic sources on the seasonal variation in the molecular composition of urban organic aerosols: a field and laboratory study using ultra-high-resolution mass spectrometry, *Atmospheric Chemistry and Physics*, 19(9), 5973-5991, https://doi.org/10.5194/acp-19-5973-2019

Darer, A. I., Cole-Filipiak, N. C., O'Connor, A. E., &Elrod, M. J. (2011). Formation and Stability of Atmospherically Relevant Isoprene-Derived Organosulfates and Organonitrates, *Environmental Science & Technology*, 45(5), 1895-1902, https://doi.org/10.1021/es103797z

Fan, W., Chen, T., Zhu, Z., Zhang, H., Qiu, Y., &Yin, D. (2022a). A review of secondary organic aerosols formation focusing on organosulfates and organic nitrates, *Journal of Hazardous Materials*, 430(128406, https://doi.org/https://doi.org/10.1016/j.jhazmat.2022.128406

Fan, W., Chen, T., Zhu, Z., Zhang, H., Qiu, Y., &Yin, D. (2022b). A review of secondary organic aerosols formation focusing on organosulfates and organic nitrates, *Journal of Hazardous Materials*, 430(https://doi.org/10.1016/j.jhazmat.2022.128406

Fu, T.-M., Jacob, D. J., Wittrock, F., Burrows, J. P., Vrekoussis, M., &Henze, D. K. (2008). Global budgets of atmospheric glyoxal and methylglyoxal, and implications for formation of secondary organic aerosols, *Journal of Geophysical Research-Atmospheres*, 113(D15), https://doi.org/10.1029/2007jd009505

Gao, Y., Wang, H., Zhang, X., Jing, S. a., Peng, Y., Qiao, L., et al. (2019). Estimating Secondary Organic Aerosol Production from Toluene Photochemistry in a Megacity of China, *Environmental Science & Technology*, 53(15), 8664-8671, https://doi.org/10.1021/acs.est.9b00651

Gilman, J. B., Lerner, B. M., Kuster, W. C., Goldan, P. D., Warneke, C., Veres, P. R., et al. (2015). Biomass burning emissions and potential air quality impacts of volatile organic compounds and other trace gases from fuels common in the US, *Atmospheric Chemistry and Physics*, 15(24), 13915-13938, https://doi.org/10.5194/acp-15-13915-2015

https://doi.org/10.5194/egusphere-2026-2472
Preprint. Discussion started: 13 May 2026

Guenther, A. B., Jiang, X., Heald, C. L., Sakulyanontvittaya, T., Duhl, T., Emmons, L. K., et al. (2012). The Model of Emissions of Gases and Aerosols from Nature version 2.1 (MEGAN2.1): an extended and updated framework for modeling biogenic emissions, *Geosci. Model Dev.*, 5(6), 1471-1492, https://doi.org/10.5194/gmd-5-1471-2012

Guo, H., Xu, L., Bougiatioti, A., Cerully, K. M., Capps, S. L., Hite, J. R., Jr., et al. (2015). Fine-particle water and pH in the southeastern United States, *Atmospheric Chemistry and Physics*, 15(9), 5211-5228, https://doi.org/10.5194/acp-15-5211-2015

Hamilton, J. F., Bryant, D. J., Edwards, P. M., Ouyang, B., Bannan, T. J., Mehra, A., et al. (2021). Key Role of NO3 Radicals in the Production of Isoprene Nitrates and Nitrooxyorganosulfates in Beijing, *Environmental Science & Technology*, 55(2), 842-853, https://doi.org/10.1021/acs.est.0c05689

Han, Y., Wang, T., Li, R., Fu, H., Duan, Y., Gao, S., et al. (2023a). Measurement report: Volatile organic compound characteristics of the different land-use types in Shanghai: spatiotemporal variation, source apportionment and impact on secondary formations of ozone and aerosol, *Atmos. Chem. Phys.*, 23(4), 2877-2900, https://doi.org/10.5194/acp-23-2877-2023

Han, Y., Zhang, X., Li, L., Lin, Y., Zhu, C., Zhang, N., et al. (2023b). Enhanced Production of Organosulfur Species during a Severe Winter Haze Episode in the Guanzhong Basin of Northwest China, *Environmental Science & Technology*, https://doi.org/10.1021/acs.est.3c02914

Hansen, A. M. K., Hong, J., Raatikainen, T., Kristensen, K., Ylisirnio, A., Virtanen, A., et al. (2015). Hygroscopic properties and cloud condensation nuclei activation of limonene-derived organosulfates and their mixtures with ammonium sulfate, *Atmospheric Chemistry and Physics*, 15(24), 14071-14089, https://doi.org/10.5194/acp-15-14071-2015

Hatch, L. E., Creamean, J. M., Ault, A. P., Surratt, J. D., Chan, M. N., Seinfeld, J. H., et al. (2011). Measurements of isoprene-derived organosulfates in ambient aerosols by aerosol time-of-flight mass spectrometry-part 2: temporal variability and formation mechanisms, *Environmental Science & Technology*, 45(20), 8648-8655, https://doi.org/10.1021/es2011836

He, S., Chen, Z., &Zhang, X. (2011). Photochemical reactions of methyl and ethyl nitrate: a dual role for alkyl nitrates in the nitrogen cycle, *Environmental Chemistry*, 8(6), 529-542, https://doi.org/10.1071/en10004

Hennigan, C. J., Izumi, J., Sullivan, A. P., Weber, R. J., &Nenes, A. (2015). A critical evaluation of proxy methods used to estimate the acidity of atmospheric particles, *Atmospheric Chemistry and Physics*, 15(5), 2775-2790, https://doi.org/10.5194/acp-15-2775-2015

Hettiyadura, A. P. S., Stone, E. A., Kundu, S., Baker, Z., Geddes, E., Richards, K., et al. (2015). Determination of atmospheric organosulfates using HILIC chromatography with MS detection, *Atmospheric Measurement Techniques*, 8(6), 2347-2358, https://doi.org/10.5194/amt-8-2347-2015

Hu, M., Krauss, M., Brack, W., &Schulze, T. (2016). Optimization of LC-Orbitrap-HRMS acquisition and MZmine 2 data processing for nontarget screening of environmental samples using design of experiments, *Analytical and Bioanalytical Chemistry*, 408(28), 7905-7915, https://doi.org/10.1007/s00216-016-9919-8

Huang, L., Cochran, R. E., Coddens, E. M., &Grassian, V. H. (2018). Formation of Organosulfur Compounds through Transition Metal Ion-Catalyzed Aqueous Phase Reactions, *Environmental Science & Technology Letters*, 5(6), 315-321, https://doi.org/10.1021/acs.estlett.8b00225

Jiang, H., Cai, J., Feng, X., Chen, Y., Guo, H., Mo, Y., et al. (2025). Organosulfur Compounds: A Non-Negligible Component Affecting the Light Absorption of Brown Carbon During North China Haze Events, *Journal of Geophysical Research: Atmospheres*, 130(1), https://doi.org/10.1029/2024jd042043

Jiang, H., Frie, A. L., Lavi, A., Chen, J. Y., Zhang, H., Bahreini, R., et al. (2019). Brown Carbon Formation from Nighttime Chemistry of Unsaturated Heterocyclic Volatile Organic Compounds, *Environmental Science & Technology Letters*, 6(3), 184-190,

https://doi.org/10.5194/egusphere-2026-2472
Preprint. Discussion started: 13 May 2026

https://doi.org/10.1021/acs.estlett.9b00017
Jiang, H., Li, J., Tang, J., Cui, M., Zhao, S., Mo, Y., et al. (2022). Molecular characteristics, sources, and formation pathways of organosulfur compounds in ambient aerosol in Guangzhou, South China, *Atmospheric Chemistry and Physics*, 22(10), 6919-6935, https://doi.org/10.5194/acp-22-6919-2022
Kellerman, A. M., Dittmar, T., Kothawala, D. N., &Tranvik, L. J. (2014). Chemodiversity of dissolved organic matter in lakes driven by climate and hydrology, *Nature Communications*, 5(1), 3804, https://doi.org/10.1038/ncomms4804
Kourtchev, I., Giorio, C., Manninen, A., Wilson, E., Mahon, B., Aalto, J., et al. (2016). Enhanced Volatile Organic Compounds emissions and organic aerosol mass increase the oligomer content of atmospheric aerosols, *Scientific Reports*, 6(1), https://doi.org/10.1038/srep35038
Kundu, S., Quraishi, T. A., Yu, G., Suarez, C., Keutsch, F. N., &Stone, E. A. (2013). Evidence and quantitation of aromatic organosulfates in ambient aerosols in Lahore, Pakistan, *Atmospheric Chemistry and Physics*, 13(9), 4865-4875, https://doi.org/10.5194/acp-13-4865-2013
Li, L., Li, J., Zhang, X., Lin, Y., Wang, R., Cao, J., et al. (2024). Effects of relative humidity on atmospheric organosulfur species derived from photooxidation and nocturnal chemistry in a forest environment, *Environmental Pollution*, 363(https://doi.org/10.1016/j.envpol.2024.125253
Li, Z., Ratliff, E. A., &Sharkey, T. D. (2011). Effect of Temperature on Postillumination Isoprene Emission in Oak and Poplar, *Plant Physiology*, 155(2), 1037-1046, https://doi.org/10.1104/pp.110.167551
Lim, Y. B., &Ziemann, P. J. (2009). Effects of Molecular Structure on Aerosol Yields from OH Radical-Initiated Reactions of Linear, Branched, and Cyclic Alkanes in the Presence of NOx, *Environmental Science & Technology*, 43(7), 2328-2334, https://doi.org/10.1021/es803389s
Lin, P., Rincon, A. G., Kalberer, M., &Yu, J. Z. (2012a). Elemental Composition of HULIS in the Pearl River Delta Region, China: Results Inferred from Positive and Negative Electrospray High Resolution Mass Spectrometric Data, *Environmental Science & Technology*, 46(14), 7454-7462, https://doi.org/10.1021/es300285d
Lin, P., Yu, J. Z., Engling, G., &Kalberer, M. (2012b). Organosulfates in humic-like substance fraction isolated from aerosols at seven locations in East Asia: a study by ultra-high-resolution mass spectrometry, *Environmental Science & Technology*, 46(24), 13118-13127, https://doi.org/10.1021/es303570v
Liu, Z., Gao, W., Yu, Y., Hu, B., Xin, J., Sun, Y., et al. (2018). Characteristics of $PM_{2.5}$ mass concentrations and chemical species in urban and background areas of China: emerging results from the CARE-China network, *Atmospheric Chemistry and Physics*, 18(12), 8849-8871, https://doi.org/10.5194/acp-18-8849-2018
Lukacs, H., Gelencser, A., Hoffer, A., Kiss, G., Horvath, K., &Hartyani, Z. (2009). Quantitative assessment of organosulfates in size-segregated rural fine aerosol, *Atmospheric Chemistry and Physics*, 9(1), 231-238, https://doi.org/10.5194/acp-9-231-2009
Ma, X., Tan, Z., Lu, K., Yang, X., Chen, X., Wang, H., et al. (2022). OH and HO2 radical chemistry at a suburban site during the EXPLORE-YRD campaign in 2018, *Atmos. Chem. Phys.*, 22(10), 7005-7028, https://doi.org/10.5194/acp-22-7005-2022
Ma, Y., Xu, X., Song, W., Geng, F., &Wang, L. (2014). Seasonal and diurnal variations of particulate organosulfates in urban Shanghai, China, *Atmospheric Environment*, 85(152-160, https://doi.org/10.1016/j.atmosenv.2013.12.017
Minerath, E. C., Casale, M. T., &Elrod, M. J. (2008). Kinetics feasibility study of alcohol sulfate esterification reactions in tropospheric aerosols, *Environmental Science & Technology*, 42(12), 4410-4415, https://doi.org/10.1021/es8004333
Minerath, E. C., &Elrod, M. J. (2009). Assessing the Potential for Diol and Hydroxy Sulfate Ester Formation from the Reaction of Epoxides in Tropospheric Aerosols, *Environmental Science & Technology*, 43(5), 1386-1392, https://doi.org/10.1021/es8029076
Nestorowicz, K., Jaoui, M., Rudzinski, K. J., Lewandowski, M., Kleindienst, T. E.,

https://doi.org/10.5194/egusphere-2026-2472
Preprint. Discussion started: 13 May 2026

Spolnik, G., et al. (2018). Chemical composition of isoprene SOA under acidic and non-acidic conditions: effect of relative humidity, *Atmospheric Chemistry and Physics*, 18(24), 18101-18121, https://doi.org/10.5194/acp-18-18101-2018

Ng, N. L., Brown, S. S., Archibald, A. T., Atlas, E., Cohen, R. C., Crowley, J. N., et al. (2017). Nitrate radicals and biogenic volatile organic compounds: oxidation, mechanisms, and organic aerosol, *Atmospheric Chemistry and Physics*, 17(3), 2103-2162, https://doi.org/10.5194/acp-17-2103-2017

Ning, C., Tang, Y., Sun, H., Wang, D., Sun, S., &Gao, Y. (2025). Molecular characteristics and formation pathways of organosulfates in atmospheric fine particles: A case study in steel industrial city during winter heating period, *Journal of Hazardous Materials*, 495(138882, https://doi.org/https://doi.org/10.1016/j.jhazmat.2025.138882

Noziere, B., Ekstrom, S., Alsberg, T., &Holmstrom, S. (2010). Radical-initiated formation of organosulfates and surfactants in atmospheric aerosols, *Geophysical Research Letters*, 37(https://doi.org/10.1029/2009gl041683

O'Brien, R. E., Laskin, A., Laskin, J., Rubitschun, C. L., Surratt, J. D., &Goldstein, A. H. (2014). Molecular characterization of S- and N-containing organic constituents in ambient aerosols by negative ion mode high-resolution Nanospray Desorption Electrospray Ionization Mass Spectrometry: CalNex 2010 field study, *J. Geophys. Res. Atmos.*, 119(22), 12706-12720, https://doi.org/10.1002/2014jd021955

Passananti, M., Kong, L., Shang, J., Dupart, Y., Perrier, S., Chen, J., et al. (2016). Organosulfate Formation through the Heterogeneous Reaction of Sulfur Dioxide with Unsaturated Fatty Acids and Long-Chain Alkenes, *Angewandte Chemie-International Edition*, 55(35), 10336-10339, https://doi.org/10.1002/anie.201605266

Rincón, A. G., Calvo, A. I., Dietzel, M., &and Kalberer, M. (2012). Seasonal differences of urban organic aerosol composition – an ultra-high resolution mass spectrometry study, *Environmental Chemistry*, 9(298-319, https://doi.org/10.1071/EN12016_AC

Riva, M., Barbosa, T. D., Lin, Y. H., Stone, E. A., Gold, A., &Surratt, J. D. (2016a). Chemical characterization of organosulfates in secondary organic aerosol derived from the photooxidation of alkanes, *Atmospheric Chemistry and Physics*, 16(17), 11001-11018, https://doi.org/10.5194/acp-16-11001-2016

Riva, M., Budisulistiorini, S. H., Zhang, Z. F., Gold, A., &Surratt, J. D. (2016b). Chemical characterization of secondary organic aerosol constituents from isoprene ozonolysis in the presence of acidic aerosol, *Atmospheric Environment*, 130(5-13, https://doi.org/10.1016/j.atmosenv.2015.06.027

Riva, M., Tomaz, S., Cui, T., Lin, Y.-H., Perraudin, E., Gold, A., et al. (2015). Evidence for an unrecognized secondary anthropogenic source of organosulfates and sulfonates: gas-phase oxidation of polycyclic aromatic hydrocarbons in the presence of sulfate aerosol, *Environmental Science & Technology*, 49(11), 6654-6664, https://doi.org/10.1021/acs.est.5b00836

Schindelka, J., Iinuma, Y., Hoffmann, D., &Herrmann, H. (2013). Sulfate radical-initiated formation of isoprene-derived organosulfates in atmospheric aerosols, *Faraday Discussions*, 165(237-259, https://doi.org/10.1039/c3fd00042g

Shang, J., Passananti, M., Dupart, Y., Ciuraru, R., Tinel, L., Rossignol, S., et al. (2016). SO2 Uptake on Oleic Acid: A New Formation Pathway of Organosulfur Compounds in the Atmosphere, *Environmental Science & Technology Letters*, 3(2), 67-72, https://doi.org/10.1021/acs.estlett.6b00006

Song, J., Li, M., Jiang, B., Wei, S., Fan, X., &Peng, P. (2018a). Molecular Characterization of Water-Soluble Humic like Substances in Smoke Particles Emitted from Combustion of Biomass Materials and Coal Using Ultrahigh-Resolution Electrospray Ionization Fourier Transform Ion Cyclotron Resonance Mass Spectrometry, *Environmental Science & Technology*, 52(5), 2575–2585, https://doi.org/10.1021/acs.est.7b06126

Song, S., Gao, M., Xu, W., Shao, J., Shi, G., Wang, S., et al. (2018b). Fine-particle pH for Beijing winter haze as inferred from different thermodynamic equilibrium models, *Atmospheric Chemistry and Physics*, 18(10), 7423-7438,

https://doi.org/10.5194/egusphere-2026-2472
Preprint. Discussion started: 13 May 2026

https://doi.org/10.5194/acp-18-7423-2018

Surratt, J. D., Chan, A. W. H., Eddingsaas, N. C., Chan, M., Loza, C. L., Kwan, A. J., et al. (2010). Reactive intermediates revealed in secondary organic aerosol formation from isoprene, *Proceedings of the National Academy of Sciences of the United States of America*, 107(15), 6640-6645, https://doi.org/10.1073/pnas.0911114107

Surratt, J. D., Gomez-Gonzalez, Y., Chan, A. W. H., Vermeylen, R., Shahgholi, M., Kleindienst, T. E., et al. (2008). Organosulfate formation in biogenic secondary organic aerosol, *Journal of Physical Chemistry A*, 112(36), 8345-8378, https://doi.org/10.1021/jp802310p

Tang, J., Li, J., Su, T., Han, Y., Mo, Y., Jiang, H., et al. (2020a). Molecular compositions and optical properties of dissolved brown carbon in biomass burning, coal combustion, and vehicle emission aerosols illuminated by excitation–emission matrix spectroscopy and Fourier transform ion cyclotron resonance mass spectrometry analysis, *Atmos. Chem. Phys.*, 20(4), 2513-2532, https://doi.org/10.5194/acp-20-2513-2020

Tang, J., Li, J., Su, T., Han, Y., Mo, Y. Z., Jiang, H. X., et al. (2020b). Molecular compositions and optical properties of dissolved brown carbon in biomass burning, coal combustion, and vehicle emission aerosols illuminated by excitation-emission matrix spectroscopy and Fourier transform ion cyclotron resonance mass spectrometry analysis, *Atmospheric Chemistry and Physics*, 20(4), 2513-2532, https://doi.org/10.5194/acp-20-2513-2020

Tao, S., Lu, X., Levac, N., Bateman, A. P., Nguyen, T. B., Bones, D. L., et al. (2014). Molecular characterization of organosulfates in organic aerosols from Shanghai and Los Angeles urban areas by nanospray-desorption electrospray ionization high-resolution mass spectrometry, *Environmental Science & Technology*, 48(18), 10993-11001, https://doi.org/10.1021/es5024674

Thomas, A. E., Glicker, H. S., Guenther, A. B., Seco, R., Bustillos, O. V., Tota, J., et al. (2025). Seasonal investigation of ultrafine-particle organic composition in an eastern Amazonian rainforest, *Atmospheric Chemistry and Physics*, 25(2), 959-977, https://doi.org/10.5194/acp-25-959-2025

Tolocka, M. P., &Turpin, B. (2012). Contribution of organosulfur compounds to organic aerosol mass, *Environmental Science & Technology*, 46(15), 7978-7983, https://doi.org/10.1021/es300651v

Tong, H., Kourtchev, I., Pant, P., Keyte, I. J., O'Connor, I. P., Wenger, J. C., et al. (2016). Molecular composition of organic aerosols at urban background and road tunnel sites using ultra-high resolution mass spectrometry, *Faraday Discuss*, 189(51-68, https://doi.org/10.1039/c5fd00206k

Turpin, B. J., &Lim, H. J. (2001). Species contributions to $PM_{2.5}$ mass concentrations: revisiting common assumptions for estimating organic mass, *Aerosol Science and Technology*, 35(1), r602-610, https://doi.org/10.1080/02786820152051454

Wang, D., Shen, Z., Yang, X., Huang, S., Luo, Y., Bai, G., et al. (2024a). Insight into the Role of NH_3/NH_4^+ and NO_x/NO_3^- in the Formation of Nitrogen-Containing Brown Carbon in Chinese Megacities, *Environmental Science & Technology*, 58(9), 4281-4290, https://doi.org/10.1021/acs.est.3c10374

Wang, H., Chen, X., Lu, K., Hu, R., Li, Z., Wang, H., et al. (2020a). NO3 and N2O5 chemistry at a suburban site during the EXPLORE-YRD campaign in 2018, *Atmospheric Environment*, 224(117180, https://doi.org/https://doi.org/10.1016/j.atmosenv.2019.117180

Wang, K., Huang, R.-J., Brüggemann, M., Zhang, Y., Yang, L., Ni, H., et al. (2021a). Urban organic aerosol composition in eastern China differs from north to south: molecular insight from a liquid chromatography–mass spectrometry (Orbitrap) study, *Atmospheric Chemistry and Physics*, 21(11), 9089-9104, https://doi.org/10.5194/acp-21-9089-2021

Wang, K., Zhang, Y., Huang, R.-J., Cao, J., &Hoffman, T. (2018a). UHPLC-Orbitrap mass spectrometric characterization of organic aerosol from a central European city (Mainz, Germany) and a Chinese megacity (Beijing), *Atmospheric Environment*, 189(22-29, https://doi.org/10.1016/j.atmosenv.2018.06.036

https://doi.org/10.5194/egusphere-2026-2472
Preprint. Discussion started: 13 May 2026

Wang, K., Zhang, Y., Huang, R. J., Wang, M., Ni, H., Kampf, C. J., et al. (2019). Molecular Characterization and Source Identification of Atmospheric Particulate Organosulfates Using Ultrahigh Resolution Mass Spectrometry, *Environmental Science & Technology*, 53(11), 6192-6202, https://doi.org/10.1021/acs.est.9b02628

Wang, K., Zhang, Y., Tong, H., Han, J., Fu, P., Huang, R.-J., et al. (2024b). Molecular-Level Insights into the Relationship between Volatility of Organic Aerosol Constituents and PM2.5 Air Pollution Levels: A Study with Ultrahigh-Resolution Mass Spectrometry, *Environmental Science & Technology*, https://doi.org/10.1021/acs.est.3c10662

Wang, X., Hayeck, N., Brueggemann, M., Yao, L., Chen, H., Zhang, C., et al. (2017). Chemical characteristics of organic aerosols in shanghai: a study by ultrahigh-performance liquid chromatography coupled with Orbitrap mass spectrometry, *Journal of Geophysical Research-Atmospheres*, 122(21), 11703-11722, https://doi.org/10.1002/2017jd026930

Wang, X. K., Rossignol, S., Ma, Y., Yao, L., Wang, M. Y., Chen, J. M., et al. (2016). Molecular characterization of atmospheric particulate organosulfates in three megacities at the middle and lower reaches of the Yangtze River, *Atmospheric Chemistry and Physics*, 16(4), 2285-2298, https://doi.org/10.5194/acp-16-2285-2016

Wang, Y., Hu, M., Guo, S., Wang, Y., Zheng, J., Yang, Y., et al. (2018b). The secondary formation of organosulfates under interactions between biogenic emissions and anthropogenic pollutants in summer in Beijing, *Atmospheric Chemistry and Physics*, 18(14), 10693-10713, https://doi.org/10.5194/acp-18-10693-2018

Wang, Y., Hu, M., Wang, Y.-C., Li, X., Fang, X., Tang, R., et al. (2020b). Comparative Study of Particulate Organosulfates in Contrasting Atmospheric Environments: Field Evidence for the Significant Influence of Anthropogenic Sulfate and NOx, *Environmental Science & Technology Letters*, 7(11), 787-794, https://doi.org/10.1021/acs.estlett.0c00550

Wang, Y., Takeuchi, M., Wang, S., Nizkorodov, S. A., France, S., Eris, G., et al. (2023). Photolysis of Gas-Phase Atmospherically Relevant Monoterpene-Derived Organic Nitrates, *The Journal of Physical Chemistry A*, 127(4), 987-999, https://doi.org/10.1021/acs.jpca.2c04307

Wang, Y., Zhao, Y., Wang, Y., Yu, J.-Z., Shao, J., Liu, P., et al. (2021b). Organosulfates in atmospheric aerosols in Shanghai, China: seasonal and interannual variability, origin, and formation mechanisms, *Atmospheric Chemistry and Physics*, 21(4), 2959-2980, https://doi.org/10.5194/acp-21-2959-2021

Weber, R. J., Guo, H., Russell, A. G., &Nenes, A. (2016). High aerosol acidity despite declining atmospheric sulfate concentrations over the past 15 years, *Nature Geoscience*, 9(4), 282-285, https://doi.org/10.1038/ngeo2665

Willoughby, A. S., Wozniak, A. S., &Hatcher, P. G. (2014). A molecular-level approach for characterizing water-insoluble components of ambient organic aerosol particulates using ultrahigh-resolution mass spectrometry, *Atmos. Chem. Phys.*, 14(18), 10299-10314, https://doi.org/10.5194/acp-14-10299-2014

Wu, X., Kong, Q., Lan, Y., Sng, J., &Yu, L. E. (2024). Refined Sea Salt Markers for Coastal Cities Facilitating Quantification of Aerosol Aging and PM2.5 Apportionment, *Environmental Science & Technology*, 58(19), 8432-8443, https://doi.org/10.1021/acs.est.3c10142

Xing, L., Fu, T. M., Cao, J. J., Lee, S. C., Wang, G. H., Ho, K. F., et al. (2013). Seasonal and spatial variability of the OM/OC mass ratios and high regional correlation between oxalic acid and zinc in Chinese urban organic aerosols, *Atmospheric Chemistry and Physics*, 13(8), 4307-4318, https://doi.org/10.5194/acp-13-4307-2013

Xu, L., Guo, H., Boyd, C. M., Klein, M., Bougiatioti, A., Cerully, K. M., et al. (2015). Effects of anthropogenic emissions on aerosol formation from isoprene and monoterpenes in the southeastern United States, *Proceedings of the National Academy of Sciences of the United States of America*, 112(32), E4509-E4509, https://doi.org/10.1073/pnas.1512279112

Yang, T., Xu, Y., Ma, Y.-J., Wang, Y.-C., Yu, J. Z., Sun, Q.-B., et al. (2024). Field

https://doi.org/10.5194/egusphere-2026-2472
Preprint. Discussion started: 13 May 2026

Evidence for Constraints of Nearly Dry and Weakly Acidic Aerosol Conditions on the Formation of Organosulfates, *Environmental Science & Technology Letters*, https://doi.org/10.1021/acs.estlett.4c00522

Yang, T., Xu, Y., Wang, Y. C., Ma, Y. J., Xiao, H. W., Xiao, H., et al. (2025). Non-biogenic sources are an important but overlooked contributor to aerosol isoprene-derived organosulfates during winter in northern China, *Atmos. Chem. Phys.*, 25(5), 2967-2978, https://doi.org/10.5194/acp-25-2967-2025

Yang, T., Xu, Y., Ye, Q., Ma, Y.-J., Wang, Y.-C., Yu, J.-Z., et al. (2023). Spatial and diurnal variations of aerosol organosulfates in summertime Shanghai, China: potential influence of photochemical processes and anthropogenic sulfate pollution, *Atmospheric Chemistry and Physics*, 23(20), 13433-13450, https://doi.org/10.5194/acp-23-13433-2023

Yao, M., Zhao, Y., Hu, M., Huang, D., Wang, Y., Yu, J. Z., et al. (2019). Multiphase Reactions between Secondary Organic Aerosol and Sulfur Dioxide: Kinetics and Contributions to Sulfate Formation and Aerosol Aging, *Environmental Science & Technology Letters*, 6(12), 768-774, https://doi.org/10.1021/acs.estlett.9b00657

Yassine, M. M., Harir, M., Dabek-Zlotorzynska, E., &Schmitt-Kopplin, P. (2014). Structural characterization of organic aerosol using Fourier transform ion cyclotron resonance mass spectrometry: aromaticity equivalent approach, *Rapid Commun Mass Spectrom*, 28(22), 2445-54, https://doi.org/10.1002/rcm.7038

Ye, J. H., Abbatt, J. P. D., &Chan, A. W. H. (2018). Novel pathway of SO2 oxidation in the atmosphere: reactions with monoterpene ozonolysis intermediates and secondary organic aerosol, *Atmospheric Chemistry and Physics*, 18(8), 5549-5565, https://doi.org/10.5194/acp-18-5549-2018

Yee, L. D., Craven, J. S., Loza, C. L., Schilling, K. A., Ng, N. L., Canagaratna, M. R., et al. (2013). Effect of chemical structure on secondary organic aerosol formation from C₁₂ alkanes, *Atmos. Chem. Phys.*, 13(21), 11121-11140, https://doi.org/10.5194/acp-13-11121-2013

Zhang, M., Cai, D., Lin, J., Liu, Z., Li, M., Wang, Y., et al. (2024). Molecular characterization of atmospheric organic aerosols in typical megacities in China, *npj Climate and Atmospheric Science*, 7(1), 230, https://doi.org/10.1038/s41612-024-00784-1

Zhang, X., Li, L., Lin, Y., Wang, R., Zhu, C., Xiao, S., et al. (2025). Chemical Diversity of Organosulfur Species in Various Atmospheric Environments Over the Guanzhong Basin of Northwest China, *Journal of Geophysical Research: Atmospheres*, 130(7), e2024JD042478, https://doi.org/https://doi.org/10.1029/2024JD042478

Zhao, X., Hu, Q., Wang, X., Ding, X., He, Q., Zhang, Z., et al. (2015). Composition profiles of organic aerosols from Chinese residential cooking: case study in urban Guangzhou, south China, *Journal of Atmospheric Chemistry*, 72(1), 1-18, https://doi.org/10.1007/s10874-015-9298-0

Zhu, M., Jiang, B., Li, S., Yu, Q., Yu, X., Zhang, Y., et al. (2019). Organosulfur Compounds Formed from Heterogeneous Reaction between SO2 and Particulate-Bound Unsaturated Fatty Acids in Ambient Air, *Environmental Science & Technology Letters*, 6(6), 318-322, https://doi.org/10.1021/acs.estlett.9b00218

https://doi.org/10.5194/egusphere-2026-2472
Preprint. Discussion started: 13 May 2026

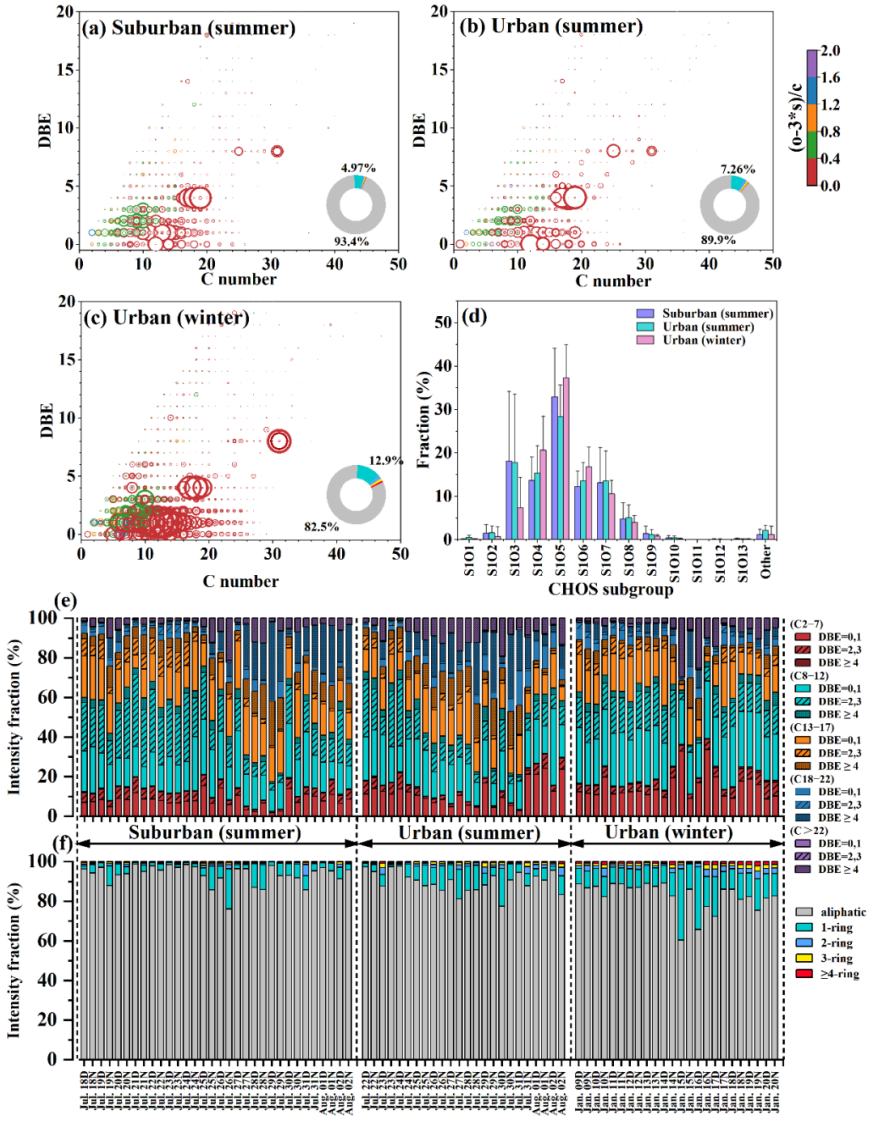

Figure 1 Molecular distribution of CHOS compounds detected by Orbitrap MS for the $PM_{2.5}$ samples collected in the three field campaigns. (a–c) Double-bond equivalent (DBE) *vs* C number for all the CHONS compounds in the suburban (summer) and urban (summer, winter). The circle area is proportional to the square root of the relative abundance of individual molecules, and the color bar denotes the degree of oxidation. (d) Classification of CHOS species into different subgroups according to the numbers of S and O atoms in their molecules. (e) Percentages of the intensity of each subgroup divided based on the DBE value and the length of carbon skeleton in the formulas. (f) Intensity percentages of each subgroup which were divided based on the Xc value of formulas.

https://doi.org/10.5194/egusphere-2026-2472
Preprint. Discussion started: 13 May 2026

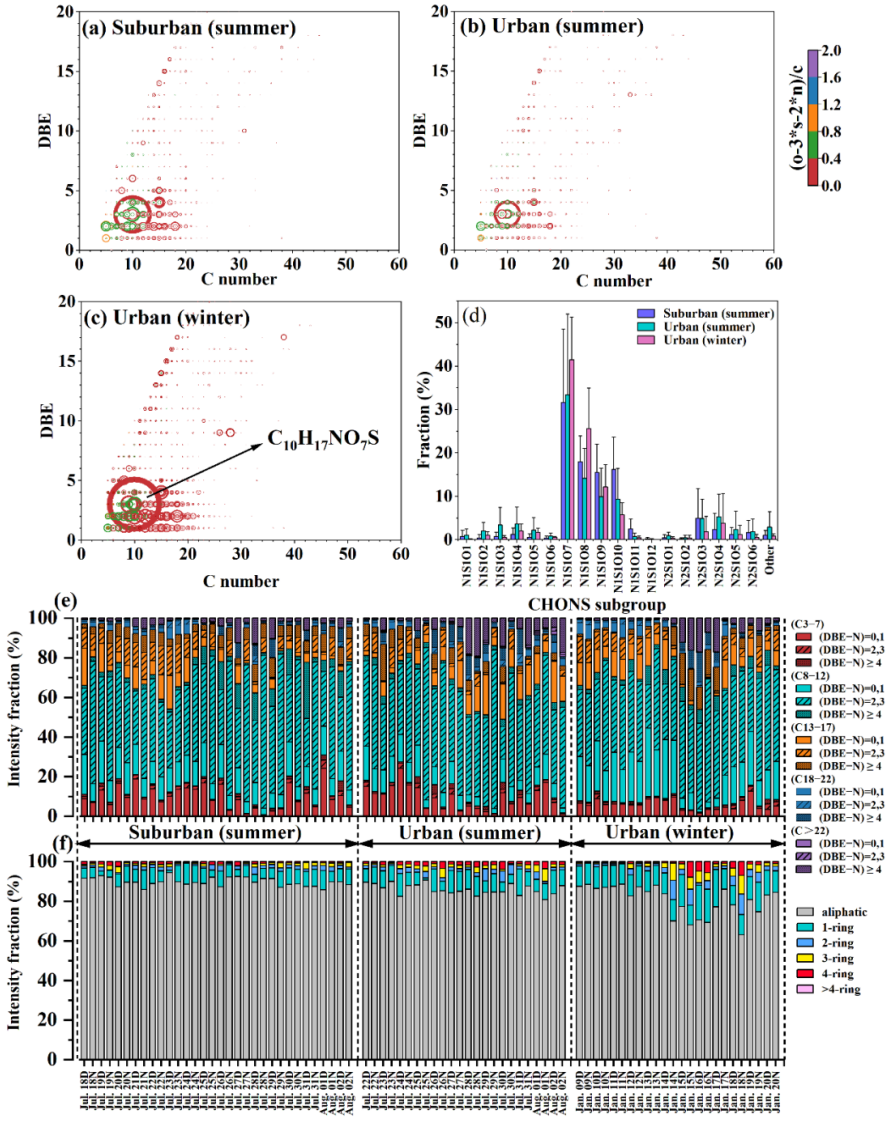

Figure 2 Molecular distribution of CHONS compounds detected by Orbitrap MS for the $PM_{2.5}$ samples collected in the three field campaigns. (a−c) Double-bond equivalent (DBE) *vs* C number for all the CHONS compounds in the suburban (summer) and urban (summer, winter). The circle area is proportional to the square root of the relative abundance of individual molecules, and the color bar denotes the degree of oxidation. Several of the most abundant CHONS species listed in descending order by their average intensities in (a) are $C_9H_{15}NO_8S$, $C_{10}H_{17}NO_7S$, $C_{10}H_{17}NO_8S$, $C_{10}H_{17}NO_9S$, $C_{10}H_{17}NO_{10}S$, and $C_{15}H_{25}NO_7S$ (Figure S4). (d) Classification of CHONS species into different subgroups according to the numbers of S and O atoms in their molecules. (e) Percentages of the intensity of each subgroup divided based on the (DBE−N) value and the length of carbon skeleton in the formulas. (f) Intensity percentages of each subgroup which were divided based on the Xc value of formulas.

https://doi.org/10.5194/egusphere-2026-2472
Preprint. Discussion started: 13 May 2026

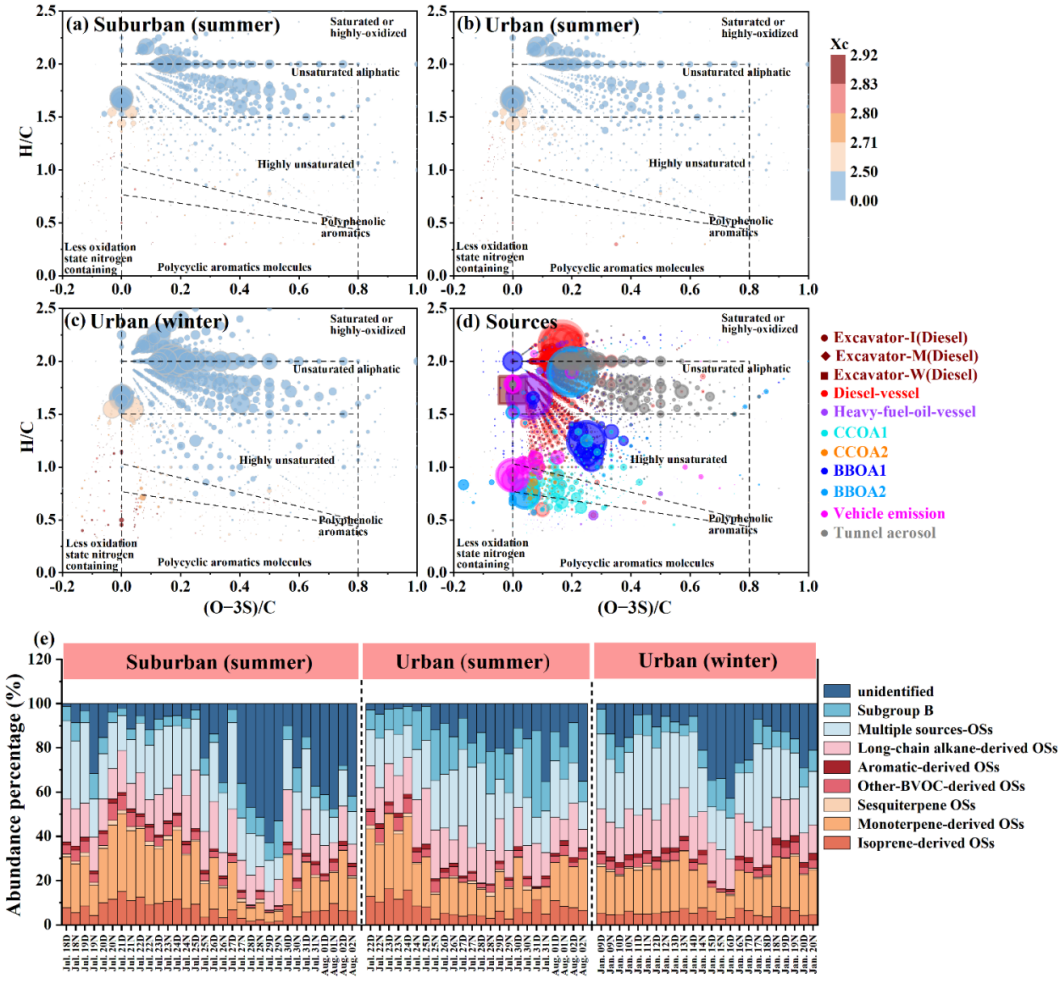

Figure 3 (a–d) Van Krevelen diagrams of CHOS for the field samples collected in Shanghai (a–c) and source samples (d) obtained from Cui et al. (2019) and Tang et al. (2020), including biomass burning organic aerosols (BBOAs), coal combustion organic aerosols (CCOAs), vehicle emissions, tunnel aerosols, and off-road engine emissions (excavator and vessel). Excavator-I, -M, and -W denote the operation modes of idling, moving, and working respectively. The circle area is proportional to the square root of the relative abundance of individual molecules in Figure 3 (a–c) The marker size denotes the percentages of MS intensity to the total identified CHOS compounds in Figure 3d. (e) Spatial, seasonal, and diurnal variations of potential precursors of detected OSs to the total intensity of identified CHOS species; subgroup B denotes OSs with unidentified precursors that satisfy $C > 8$, $DBE < 3$ and $3 < O < 7$, whereas "unidentified" denotes NOSs with unidentified precursors that fall outside these criteria.

https://doi.org/10.5194/egusphere-2026-2472
Preprint. Discussion started: 13 May 2026

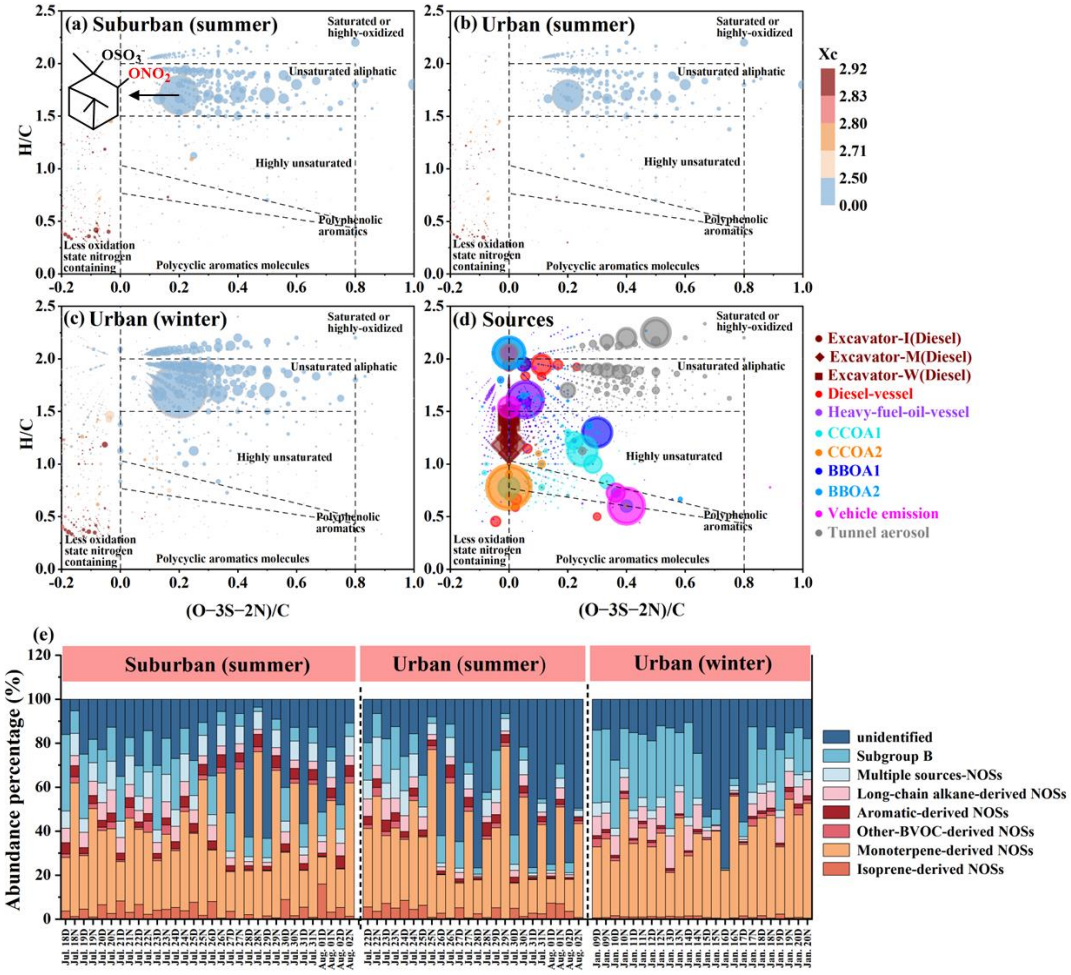

Figure 4 (a−d) Van Krevelen diagrams of CHONS for the field samples collected in Shanghai (a−c) and source samples (d) obtained from Cui et al. (2019) and Tang et al. (2020), including biomass burning organic aerosols (BBOAs), coal combustion organic aerosols (CCOAs), vehicle emissions, tunnel aerosols, and off-road engine emissions (excavator and vessel). Excavator-I, -M, and -W denote the operation modes of idling, moving, and working respectively. The circle area is proportional to the square root of the relative abundance of individual molecules in Figure 4 (a−c) The marker size denotes the percentages of MS intensity to the total identified CHONS compounds in Figure 4d. (e) Spatial, seasonal, and diurnal variations of potential precursors of detected NOSs to the total intensity of identified CHONS species; subgroup B denotes NOSs with unidentified precursors that satisfy C > 8, DBE < 3 and 6 < O < 10, whereas “unidentified” denotes NOSs with unidentified precursors that fall outside these criteria.

https://doi.org/10.5194/egusphere-2026-2472
Preprint. Discussion started: 13 May 2026

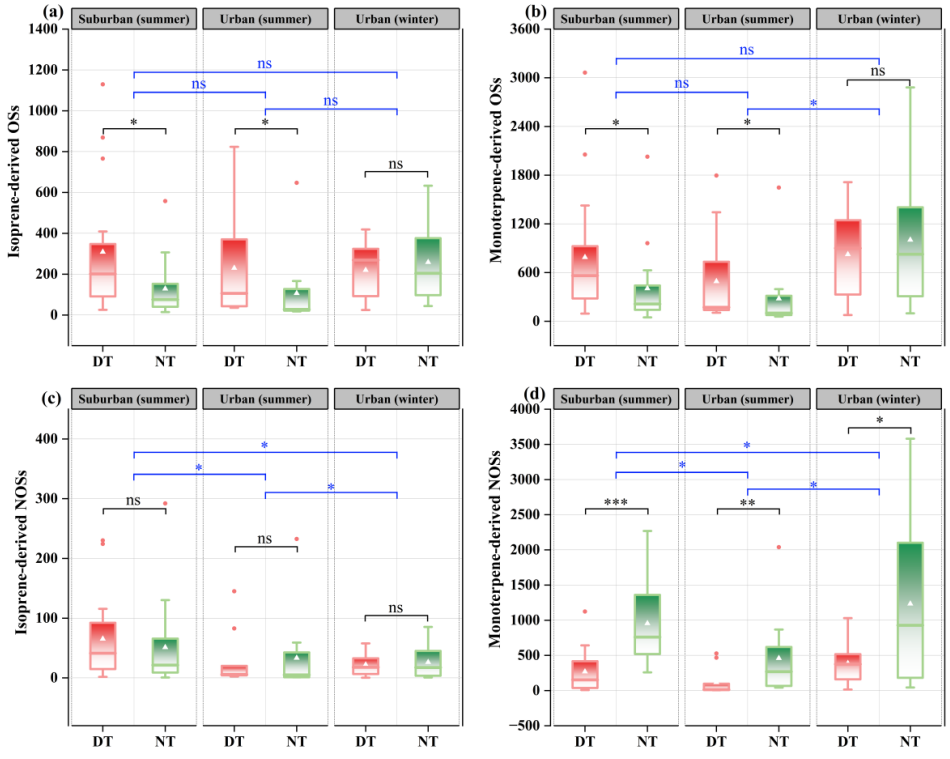

Figure 5. Spatial, seasonal, and diurnal variability of isoprene- and monoterpene-derived OSs (a, b) and NOSs (c, d). The y-axis represents the relative abundances of monoterpene/isoprene-derived OSs and NOSs, defined as peak areas normalized to the internal standard. The whisker plot boundaries are between the 10th and 90th percentiles, the box displays the 25th, 50th (median), and 75th percentiles, and the triangles display the mean values. Asterisks denote statistical significance (* $p < 0.05$, ** $p < 0.01$, *** $p < 0.001$), while "ns" indicates no significance.

https://doi.org/10.5194/egusphere-2026-2472
Preprint. Discussion started: 13 May 2026

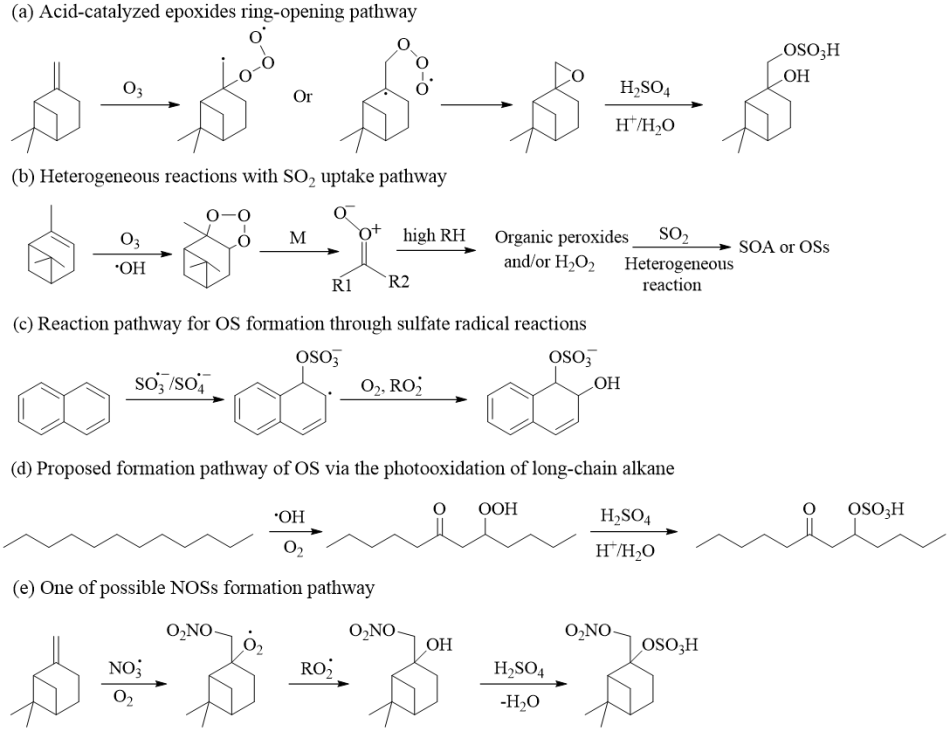

Figure 6. Potential formation mechanisms of OSs and NOSs in Shanghai (Brüggemann et al., 2020; Bruggemann et al., 2020; Surratt et al., 2008; Ye et al., 2018). (a) Proposed OSs formation pathway for acid-catalyzed ring-opening of epoxides. (b) Proposed OSs formation pathway for ozonolysis of unsaturated hydrocarbon in the presence of SO_2 at high relative humidity. (c) Reaction pathway for OSs formation through sulfate radical reactions. (d) One of the possible OSs formation pathways by long-chain alkanes (Riva et al., 2016). (e) One of the possible NOSs formation pathways.

https://doi.org/10.5194/egusphere-2026-2472
Preprint. Discussion started: 13 May 2026

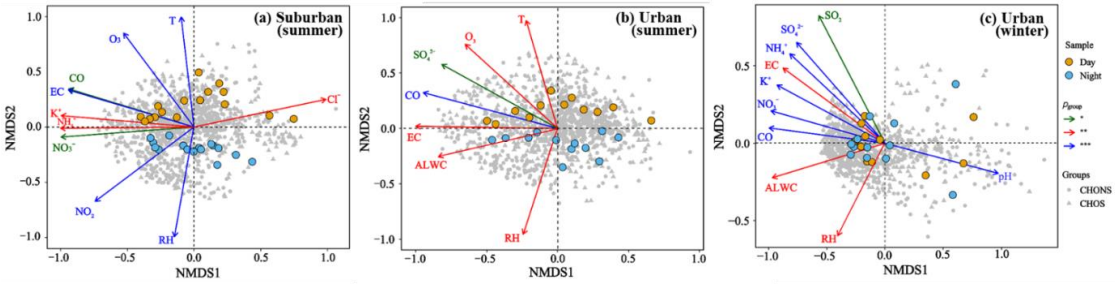

Figure 7. Nonmetric multidimensional scaling (NMDS) analysis of environmental drivers for the molecular distributions of organosulfur compounds in suburban summer (a), urban summer (b), and urban winter (c). The two-dimensional ordinations are based on Bray–Curtis dissimilarity (stress < 0.15, nonlinear $r^2 = 0.99$) using sum-normalized intensities of individual compounds. Gray triangles and circles represent CHOS and CHONS compounds, respectively. Only significant environmental variables are shown, with color-coded vectors indicating levels of significance: $p < 0.05$ (green), $p < 0.01$ (red), and $p < 0.001$ (blue).